August 2013 - Vol:3 No:1

International JOURNAL of SEWC

Structural Engineers World Congress

ISSN 2249-183X

HISTORY OF STRUCTURAL ENGINEERS WORLD CONGRESS Inc. (SEWC Inc.)

Here are a few important points taken from the paper on " Structural Engineers World Congress Idea to Reality" by Roland L. Sharpe, Founding President SEWC Inc.

Informal discussions in the mid 1980s between U.S. and Japanese structural engineers and researchers raised questions about the role of the structural engineer, required capabilities, and how the SE public image could be improved. Further informal meetings and mail correspondence over several years examined in some detail how this interaction could best be accomplished. These interactions led to small meetings at American Society of Civil Engineers (ASCE) Congresses in the U.S. which culminated in 1994 when six professional organizations agreed to form a coalition to sponsor and organize the first Structural Engineers World Congress (July 18 to 23, 1998) in San Francisco.

Recognition of the need for a worldwide SE Congress, need for interaction between SEs worldwide, scope and impact of SE services and effects on society, the need to improve the image and credibility of the SE grew over the next few years.

Range of SE Activities

Although several international organizations exist that serve structural engineers needs in specific areas such as bridges and buildings (IABCE), tall buildings, earthquake engineering, they do not serve many aspects of SE concerns. A consensus developed in the Task Committee that the WSC should include the full range of SE issues - technical, professional, ethics, education, legal, construction, products, and other related issues. There should be exhibits along with sessions on these topics. It also became apparent that the WSC should be "people" oriented with the theme of getting to know each other better. It was estimated that there are about 50,000 structural engineers in the U.S. and perhaps 200,000 or more in the world.

The question of who is a structural engineer was examined. As noted previously, in Japan civil engineers design bridges and other structures associated with infrastructure and mostly work for the government. This appears to be true for some other countries. It was recommended that all engineers designing and constructing structures are considered structural engineers and should be included in WSC. The Committee felt strongly that the WSC should not become a membership organization and should not compete with existing international SE organizations.

In the 1998 congress in San Francisco, there were about 1800 participants from 49 different countries. A large number of exhibitors presented their products. Subsequently in 2002, it was held in Yokohama, Japan and in 2007 in Bangalore, India. Each of the congresses in Japan and India attracted more than 1300 delegates.

The Structural Engineering World Congress (SEWC) is dedicated to the Art, Science and Practice of Structural Engineering. SEWC Congress brings all the structural engineers on a common platform at-least once in 4 years

SEWC presents excellent opportunities for Structural Engineering professionals to interact with each other and to learn more about what is happening in the World of Structural Engineering now and about the trends for the future.

August 2013 - Vol: 3 No: 1

International JOURNAL of SEWC

Structural Engineers World Congress

Content

Founding Member Organisations 2
SEWC Board Members 2
Editorial Board 2
Members 2
Guidelines to Authors 2
President's Message 3
Editorial 4

Journal Section

5 Creating Architecture with Tensile Membrane Structures
Horst Berger

11 Soap Film Models in the Form of Mobius Strip and Enneper
Hooi M. YEE, Kok K. CHOONG and Jae-Yeol KIM

15 Structural Optimization of Cable Dome Structures by using Genetic Algorithms
Byoungwook Yoon, Hyungmin Kim and Jaehong Lee

19 Seismic Response of Single Layer Latticed Cylindrical Shell Structures with Seismic Isolation System
Yukihiro Matsumoto, Seishi Yamada, Kenji Sasahara and Takeshi Seino

23 Soil Improvement Using Vibro Replacement Technique
Ali Dadashzadeh Sayar, Mohamadhasan Khalilpasha

27 Technical Characteristics of Friction Pendulum™ Bearings
Victor Zayas

38 Advanced Models for Condition Survey and Inspection Planning of RC Structures in Marine Environment
K. Balaji Rao and M. B. Anoop

Magazine Section

46 News
52 Events

Cover Picture Source: www.pressealgerie.fr

Published by: Vidyashankar Hoskere on behalf of SEWC Society, INSTRUCT, 1st Floor, UVCE Alumni Association Building, K.R. Circle, Banglore - 560 001. Email: sewcsociety@gmail.com. **Designed and Printed by:** 'The Masterbuilder', 102/11, Tripti Apartments, Marshalls Road, Egmore, Chennai - 600 008, Tamil Nadu, India. Email: editor@masterbuilder.co.in

Guidelines to Authors

Contributions resulting from original research in the area of structural Engineering, analysis, design, structural materials and other related topics in the form of technical papers to be published in the International Journal of Structural Engineers World Congress (SEWC) are welcome.

Prospective authors are free to prepare the manuscripts in their own convenient format and submit in MS Word file. The publisher will modify the format according to the standard format of the journal before printing.

The authors are requested to particularly not to miss mentioning the page number of the paper / book in the list of reference.

The manuscript submitted will be peer reviewed and the comment will be made known to the author.

President's Message

Sundaram R
President Structural Engineers World Congress, Worldwide
Member, Advisory Board, IASS

We are overwhelmed by the tremendous response and encouragement received for the last three SEWC Journals from all over the world. The fourth edition of SEWC Journal is being released now.

We are sure that our continued efforts will definitely fetch good results and we will do our best to maintain good quality of the publication in all aspects.

We will have articles covering wide range of subjects and will strive hard to make the journals accessible to more people as our aim is to help disseminate knowledge and information among the structural engineering fraternity.

SEWC India is organising an International Colloquium in New Delhi on the subject on 'Architecture-Structure' Interaction during November 18th - 20th 2013th in New Delhi and many top-notch Architects and Structural Engineers from different parts of the world are delivering Keynote speeches to share their knowledge.

Congratulations to Dr. B.K. Raghu Prasad, Editor-in-Chief, Mr. K.P. Pradeep, Editor of the Journal of SEWC and all others who have contributed for bringing out this latest Journal.

Editorial

Prof. Raghu Prasad B.K
Editor-in-Chief

Concrete structures are increasingly important in all developing countries because of rapid increase in urbanization. Concrete structures have become more popular because of new materials like self - consolidating concrete of even very high strengths like 80 MPa are possible.

Structures of very large depths are quite common particularly in tall buildings which consist of transfer girders of depths of the order of a meter and above. The present day flyovers and spans which are very large for the city metro require girders of very large depths over a meter high. The theories of analysis and design of concrete structures both with working stress and limit states do not mention about disadvantages of such large depths. The general feeling is that larger the depth, greater is the safety. However, the so called 3rd evolution in the analysis of concrete structures which is fracture mechanics does mention about size effect. Larger the size, lower is the tensile strength of concrete which is classified as quasi-brittle. Tensile strength is directly related to shear strength. Unfortunately even the codes of practice are yet to completely make recommendations about the same. In the past, there have been examples of failures of large sized structures due to absence of consideration of size effect. Sizes which are very large more than a critical value, not only have reduced tensile strengths but also fail in a brittle manner. (Compared to those obtained in a standard laboratory tests done on obviously small sized specimens)

Creating Architecture with Tensile Membrane Structures

Horst Berger

Summary

The paper first illustrates the design process of a tensile membrane structure on the recently extended covered pavilion for the Mitchell Performing Arts Center. (Fig.2). Built in 2009, it describes aspects of design and construction, and the effect on architectural space, lighting, comfort, sound and aesthetics. It then describes other major projects: the Jeddah Hajj Airport and its life span, the lightness of the King Fadh Stadium, the structural and architectural properties of the Jeppesen Terminal of the Denver airport. It touches on fabric materials and on the evolution of un-built designs. Fabric tensile structures have become a common form in today's architecture worldwide.

Keywords: tensile membrane, fabric, long span, light weight, translucency, reflectivity

Introduction

I was a student of civil engineering at Stuttgart University soon after WWII, when the city was still in ruins. Before that I had spent a year in the US, studying mainly architecture. I knew we had to build a better and more peaceful world. But I could not decide should I be an architect or an engineer. A successful young architect friend told me: study engineering, that's the best preparation for you to make a contribution in architecture. I studied engineering. And my engineering was always contributing to the creation of architecture.

Fig.1 Bridge at Mühlheimer Hafen, 1957

Fig.2 The Mitchell Performing Arts Center 2009

I was interested in the new composite materials. But when used in flexural members they were too soft. I started my carrier in the bridge design department of one of Germany's leading concrete builders. And I got to design a beautiful arch bridge: the 90 m span pedestrian bridge over the entrance to Mühlheimer Hafen in Cologne (1957). Its shape was funicular: the centerline of the bridge followed the thrust line of the structural forces under dead load. I learned everything about buckling.

And I learned how to make a compression structure thin and elegant. (Fig.1). At Severud Assoc. in New York, just a few years later, I became familiar with the power of tensile structures: while under compression a thin structural member will escape the direct force line by buckling sideways, under tension there is only one way, the straight way. You can use high strength materials and make members thin. Their stability is generated by having two intersecting force surfaces stressed against each other. (Fig.3). The structure can be amazingly light. That started my work in tensile membrane structures, The last one I designed in 2009. It was the extended roof cover of the Mitchell Pavilion (Fig.2). I was the architect and the engineer.

Without the computer the "funicular" shape of a three-dimensional tensile surface could not be defined. And the proper membrane material did not exist for permanent structures. So, in 1968, with the US Pavilion of the 1970

World Fair in Osaka as challenge, we started a new firm, Geiger Berger Assoc. in New York with the purpose of developing these novel type of fabric membrane structure.

The US Pavilion was an air-supported structure of unbelievable lightness. This was David Geiger's field of interest. I found that I did not like structures that had to be held up by a machine. Being more "conservative" my interest was in pure tensile structures. I had to built or find the math, both for formfinding and non-linear analysis, develop the structural details and procedures. And we had to find the right materials. And we had to overcome the fear owners have when confronted with a new type of building structure. After the first fabric tensile structures for the 1976 Bicentennial in Philadelphia, the development was unbelievable: one of the next structures was the Hajj Terminal of the Jeddah Airport (1980), by covering 400'000 sq.m the world's largest roof structure, then and now.

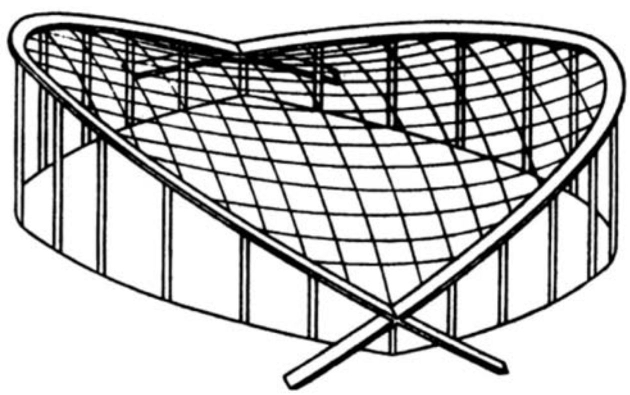

Fig.3 Raleigh Arena cable diagram. Severud Assoc. Struct. Eng.

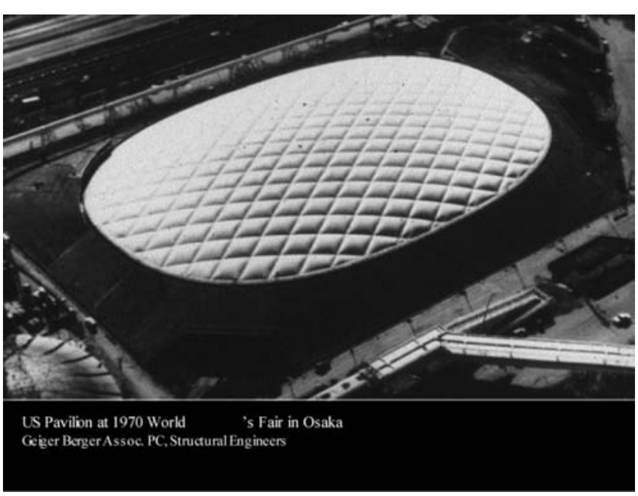

Fig.4 US Pavilion , 1970 World's Fair Geiger Berger Assoc. Struct. Eng.

The extended roof for the Mitchell Performing Arts Center, at the Woodlands near Houston, Texas

I select my latest project to illustrate the important aspects of a fabric tensile structure design. This structure opened to a sold out concert on May 1, 2009. (Fig.2, above). Because of special circumstances it had one of the fastest design and construction periods ever. The original Mitchell Pavilion was a major project for Horst Berger Partners, the firm I started in 1983 after separating from David Geiger. George Mitchell, liking my proposed designs, gave me the lead role in the design of this project, architecture and engineering. The project actually built in 1990, had 3000 seats under the roof and 10,000 seats in the lawn beyond. The Music Pavilion was very successful, and an extension was planned in 2008. Before a team had been assembled, Hurricane Ike ripped the fabric of the roof. The hurricane had wind velocities higher than the ones the roof was required to be designed for. The design team for the expanded building started working in November, construction started just a month later and was finished a few days before the opening un May 2009.

The 1990 project consisted of 3 tent shapes hung from 3 A-frames and stretched out to the periphery. (Fig.5). In the radial direction the tension forces of the stressed membrane were resisted by near horizontal struts (which also supported the space lighting, sprinklers etc.). In the ring direction the end forces are end anchored. I based the enlarged new design, covering more than 6000 seats on an extension of the same system by keeping the existing ring of A-frames and adding a second ring further out. These new A-frames became much larger and higher. The back edge is held out by the radial struts; it's held up by diagonal cables from the new A-frame tops; and it's held down by vertical tie-down cables. The area has no snow therefore wind is the governing force. Most of it is upload. The fabric, by its curvature, carries the load between ridge cables and valley cables. The ridge cables are supported by the A-frame tops, the valley cables directly by the support masts which also carry the A-frames and surround the roof drains, The two masts facing the stage also carry the follow spot light platforms.

I designed this basic configuration by a building a stretch fabric model. (Fig.6). Once we had established in the field the exact location of the new masts I built digital formfinding models of the typical fabric sections. These were intro-

Fig.5 Mitchell Performing Arts Center 1990

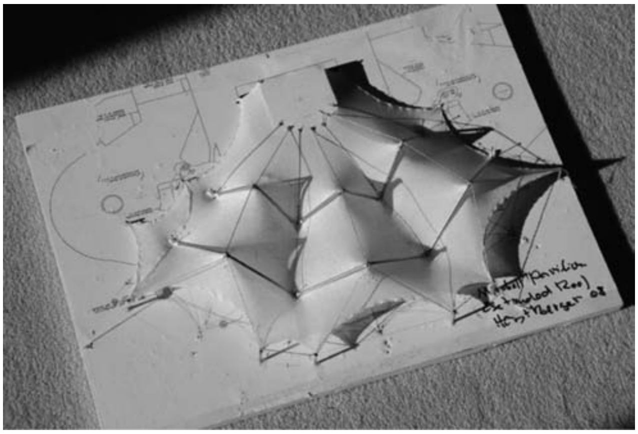

Fig.6 Stretch Fabric Model for Extended Roof 2008

duced into the SketchUp image, shared by all the members of the design team. It was even the starting point for the fabricator's patterning design of the fabric panels. This sculptural fabric shape (Figs.2,7,8) was the architecture, only amplified by reflective lights during the shows. It also acted as sound control, since the tent peaks form "black holes" for upward sound and thereby largely dampens disturbing echoes. Therefore this space works for such extremes as symphony concerts and rock music.

The fabric membrane shape is at the same time structural system, architectural space, sound system, lighting projection screen. Sitting in the space under the roof, in spite of the 6,000 seats, gives an amazing sense of intimacy. And for nearby downtown "Woodlands" it is a floating super sculpture on the hill.

And George Mitchell, the man who created "tThe Woodlands" (now a New Town of 90,000 people), and the force behind the Pavilion is happy with the result.

25 Year Award for the Jeddah Hajj Terminal: The Forest in the Desert

In 2010, the Jeddah Hajj Terminal received the AIA's 25 year award. This project was the hardest thing I ever did in

Fig. 7. Mitchell Pavilion Interior 2009

Fig. 8 Mitchell Pavilion Exterior 2009

my professional life. The largest and most complex fabric structures I had designed before were a number of pavilions for the Bicentennial Celebration in Philadelphia in 1976. An architect who worked on one of these went to SOM in New York and, when SOM began to look for a design for the Hajj Terminal, he suggested the use of a fabric structure design. I was invited to consult SOM New York on the schematic design which let to selection of a tensile fabric membrane structure solution. Later the project went to SOM Chicago where the present design evolved; a design/built concept to be completed and built by a contractor. Owens Corning Fiberglass with Birdair was the contractor, and I was their design and engineering consultant. The design consisted of 10 modules, each consisting of 21 tent units, whose form came directly from my square tent design for an animal park in New Jersey. Each of the 210 tent units was 45.75 m x 45.75 m, about the size of the largest Philadelphia structures. The Hajj Terminal, with 440,000 sq m was then, and is now, the largest roof cover in the world. We had the computer programs to handle formfinding and non-linear stress analysis of the fabric units. When we got parts or all of the overall system engaged we had to use our mathematical imagination to help us shortcut the analysis, because even the Crey computer we used in time-sharing, could not deal with the size of the system then. (Today a Macintosh laptop can handle it).

Each unit of 2100 sq m fabric came in a box of 4x8x16 ft (1.22x2.44x4.88m) and was folded so that it could be pulled out by its peak which was connected to the bottom part of a double steel ring. The upper part was hung in its final position, suspended from 8 cables that brought the load to the top of the pylons located in the four corners of each unit. The upper ring contained a winch and a jack. So all 21 tent units of each module could be brought up together close to the upper ring and than stressed together. Only the force balance kept the units in place. Therefore it was amazing that in all cases the rings lined up perfectly with the bolt holes in position so that the connection bars could be pushed through. All 10 modules were erected in 2 years.

Replacements were planned after 25 years. The structure

Fig. 9: I stand on module A, 85% stressed.1980

Fig.10: Jeddah Construction: Module A to E up in place, Module F up, G being installed

is now 30 years old, some parts 32. The Teflon coated fiberglass lasts longer in a dry climate, since the only cause of deterioration is the penetration of moisture to the ultra thin glass fibers, with the adhesion forces of the moisture reducing the strength of the glass fiber.

Though SOM claims credit for this achievement, both for its architecture and engineering, I know that this is one project that would not exist in this form without my contribution, in technology and in aesthetic detail. It was the hardest thing I ever did, as I said before, and I am proud of it. Because, in a sense, it changed the world of fabric membrane structures.

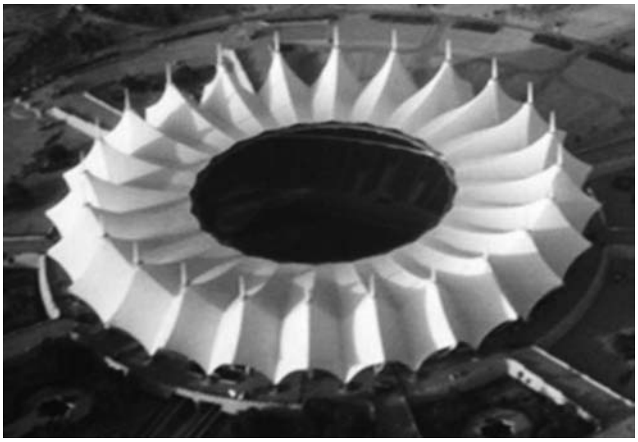

Fig.11. Riyadh Stadium from the Air

A Huge, Partially Covered, Stadium: Light and Fast Construction

The King Fadh Stadium in Riyadh, Saudi Arabia, was a direct successor of the Hajj Terminal. By now the Saudis had come to love modern tent structures and had recognized it as belonging to their own tradition. Indeed, the black tents of the Bedouins are master pieces of technology and art. They are very beautiful predecessors of modern tensile membrane structures. Because of the success of the Jeddah airport roof we were critical for this project. The stadium cover is roughly 95% of the size and span of the Beijing Olympic Stadium, but required only 3,000 tons of structural steel rather than 50,000. The entire fabric consists of two shapes and their mirror images. A large ring cable holds the entire structure together. It took little change to make the structure capable of totally enclosing this large space, which has a 290 m diameter. The huge shade area shelters the space against the desert sun. The structural engineering for the construction phase was given to Schlaich and Partner, who added valuable knowledge in cable protection and excellent design of cast-steel connection details.

Fig.12. Interior Detailed View

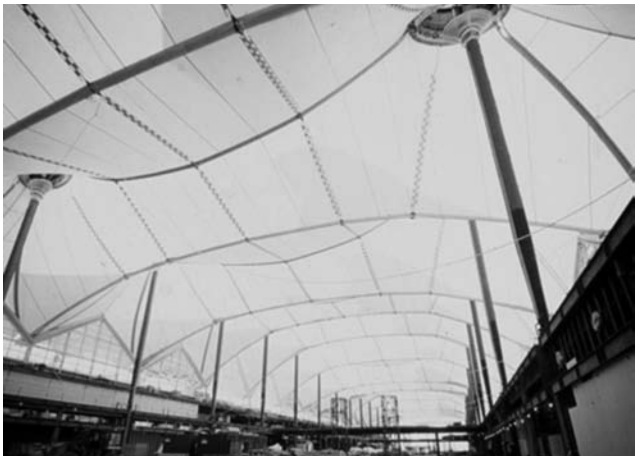

Fig.13. View of Structural Membrane

Fig. 14. Anchorage and Edge Catenaries

Fig.15. Interior View, Great Hall, Denver

The Denver International Airport: Fabric Structure for the Jeppesen Terminal,

An iImportant 24/7 Building

This is a very busy, important, regular building enclosed in translucent fabric and glass. It was built faster and works better than a conventional alternative. Inside the space has the sense of a large, very light, elegant, daylight filled cathedral. There is a real sense of sun and clouds outside.

Fig.16. Exterior View of Jeppesen Terminal, Denver

Fig.17. Silicone Coated Fiberglass Fabric at Poughkeepsie Mall. Horst Berger Part. Eng.

With 10% of daylight penetrating the translucent fabric, little artificial light is needed. Also the fabric reflects 75 % of sunlight and heat from the sun. This reduces the heat gain of the building as does the fact that in the night the translucent skin radiates out heat, so that in the morning the inside is cooler than the outdoor environment. This drastically reduces the cost of air conditioning.

The structure for the Jeppesen Terminal Building enclosure is very simple. (Fig.13). The structural fabric spans between ridge and valley cables. The ridge cables carry the load to the top of masts set 45.75m (150 ft). apart. The bays (mast spacing) are 18.3m (60 ft) wide. The valley cables hold the structure down and are anchored outside, beyond the great hall (Fig.14).

Completed in 1994 this tensile structure roof has carried record snow loads. It has a very low operating cost. And it is a very attractive architectural space that people like to be in.

The future of Fabric Membrane structures in Architecture

There are two obstacles to the more general future use of tensile membrane structures in architecture. One is the special expertise required for the design. The other is the availability of fabric which is easy to handle and has a long life span. With computer assisted design the common basis for structural design, the first problem will easily be overcome. There are easier and better formfinding programs available. And nonlinear stress analysis is quite common. Tensile structures are more widely used all over the world, making owners, architects and engineers more familiar with the specifics of the technology.

A fabric for permanent structures is already available. In the 1980s I worked with Dow Corning on the development and use of silicon coated fiberglass. Dow Corning set up a fabric structure company in Atlanta, Georgia, to which I was a consultant. We built a number of structures using the Dow Corning material. One of the structures from that

Fig. 18. Zenith Arena, Strassbourg, France Architect: Massimiliano Fuksas

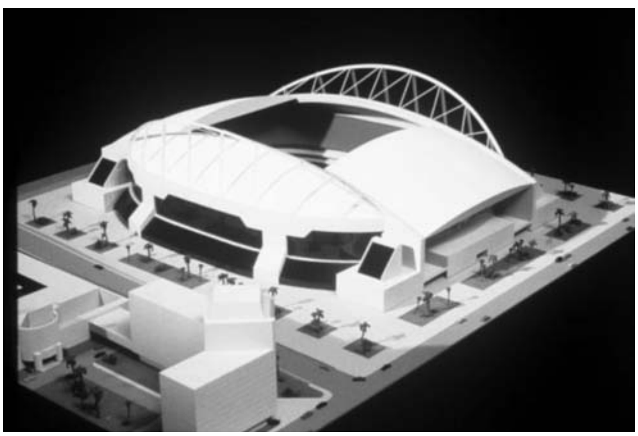

Fig.19. Retractable Roof for Phoenix Stadium Horst Berger's Design 1983

period is the roof covering the Poughkeepsie Mall in New York. Fig.17 shows a recent photograph of that roof. The fabric had two problems. The skin tended to collect dirt on the outside which could not be removed; and it was difficult to do seaming on the site. These problems have been overcome by the Atex (Fig.18) and other . This fabric should last much longer than Teflon-coated fiberglass, since the silicone will prevent the penetration of moisture which causes the weakening of the super thin glass fibers. It also has very high translucencies.

Fig.20. Retractable Roof for Dallas Cowboys Walter P. Moore's Design, built 2011

Fig. 18. Zenith Arena, Strassbourg, France Architect: Massimiliano Fuksas

There is no doubt in my mind that tensile membrane fabric structures will play a growing role in the architecture of the future.

Impact of Unbuilt Designs

I am particularly pleased by the fact that some of my designs which were never built have led to new designs used in major buildings. I will use just one example. My roof design for a stadium with a movable roof for Phoenix, Arizona (Fig.19) has led to a new solution by the structural engineering firm of Walter P.Moore using a variation of the initial concept. A second step in this evolution, a movable roof for the Dulles Cowboys (Fig.20) has even more similarity to my original concept.

Epilogue

I want to end this paper as an opportunity to express my joy and deep satisfaction for having been able to spend my professional life in the activity of building. Much of it was hard work, and some of it was quite difficult. But all of it was great, because it was engaged of making the built environment richer and more beautiful. And it was a pleasure to work with my colleagues, both engineers and architects.

At the completion of my last project , the enlarged roof for the Mitchell Center of Performing, Mr. Mitchell asked on the last day of construction to have our picture taken. (Fig.21). He said: "I asked you to make it as beautiful as the first roof, but you made it better". It is a wonderful way of finishing a building project.

Author Affiliation

Horst Berger

School of Architecture, CCNY, formerly Horst Berger Partners and Geiger Berger Assoc. New York, USA

Soap Film Models in the Form of Mobius Strip and Enneper

Hooi M. YEE[1], Kok K. CHOONG[2] and Jae-Yeol KIM[3]

Summary

This paper describes an effort to produce soap film models with boundaries corresponding to those defined by Möbius strip and Enneper minimal surfaces. Soap film models with surfaces deviating from mathematically defined minimal surfaces of Möbius strip and Enneper are shown.

Keywords: Soap film model; Möbius strip; Enneper.

1. Introduction

A soap model is used to find the soap film that minimizes area subject to appreciate constraints. Ireland [1] has presented some puzzling measurements of the tension between soap film and a solid surface. Moulton and Pelesko[2] have investigated a soap film Catenoid subjected to an axially symmetric electric field. This experimental and theoretical analysis for this Field Driven Mean Curvature Surface (FDMC) surface provides a step in understanding how electric fields interact with surfaces driven by surface tension. Such interactions may be of great benefit in micro scale systems such as Micro electro mechanical systems (MEMS) and self-assembly. Brakke[3] has treated only the area minimization problem with boundary constraints. Koiso and Palmer[4] have studied a variational problem whose solutions are a geometric model for thin films with gravity which is partially supported by a given contour. The energy functional contains surface tension, a gravitational energy, a wetting energy and the Euler-Lagrange equation can be expressed in terms of the mean curvature of the surface, the curvatures of the free boundary and a few other geometric quantities. The stability or instability of vertical planar surface bounded by two vertical lines is determined. Boudaoud and Amar[5] have studied soap film Helicoid. The vibration equation shows that the Helicoid is the stable surface when its winding number is small. The Catenoid is locally isometric to the Helicoid so that their vibration spectra are strongly related. The normal forms of the bifurcations confirm the analysis. Huff[6] has considered soap films spanning rectangular prisms with regular n-gon bases. As the number of edges n varies, there are significant changes in the qualitative properties of the spanning soap films as well as a change in the number of spanning soap films.

In this paper, form-finding of soap film is used to find surface form of fabric structures of which their boundaries correspond to shape defined by mathematical equation for the classical known minimal surface. Since the initial form of a fabric structures is preferred to be in minimal surface form for a given boundary, soap film model can be used as verification of the accuracy of the mathematically defined surface.

2. Möbius Strip and Enneper

2.1 Möbius strip

A Möbius strip of half-width W with midcircle of radius R at height z = 0 as shown in Figure 1 can be represented parametrically by the following set of equations ([7]):

$$X=\left(R+S\cos\frac{\theta}{2}\right)\cos\theta,\ Y=\left(R+S\cos\frac{\theta}{2}\right)\sin\theta,\ z=s\sin\left(\frac{\theta}{2}\right) \quad (1)$$

$$for\{S:-W,W\}\ and\ \{\theta:0,2\pi\}$$

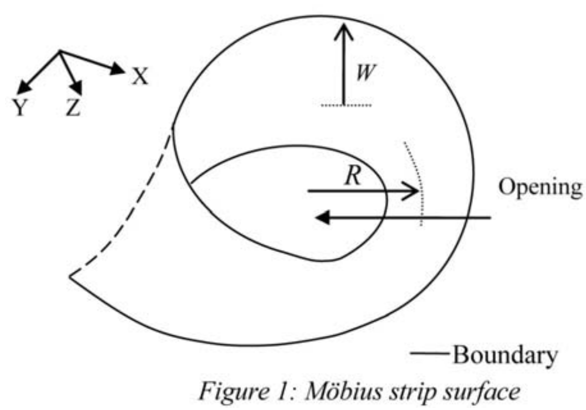

Figure 1: Möbius strip surface

2.2 Enneper

Enneper surface in Figure 2 can be obtained by using the following Equation (2) ([8]):

$$X=u-\frac{u^3}{3}+uv^2,\ Y=-v+\frac{v^3}{3}-vu^2,\ Z=u^2-v^2 \quad (2)$$

for u and v = variables.

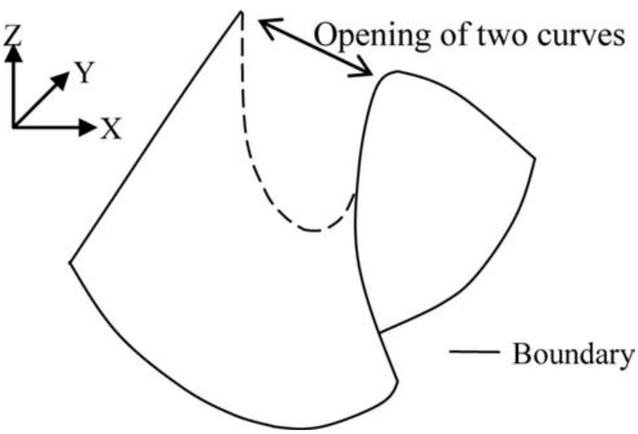

Figure 2: Enneper surface

3. Preparation of Soap Film Model

The actual size of the Möbius strip R/W=1 and R/W=2 soap film model are height, H=15cm; width, B=22.5cm and H=6.5cm; B=16cm, respectively. The actual size of the Enneper u=v=0.86 and 1.25 soap film model are H=21cm; B=12cm and H=26cm; B=16cm, respectively. The boundary of models are built using aluminum wire. Other materials used are steel, plywood, rubber band and super glue as shown in Figure 3.

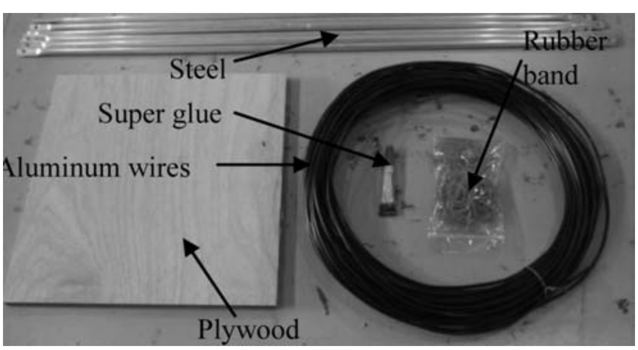

Figure 3: Materials used to build the physical model

The making of boundary frame involves the use of a wooden base where x and y coordinates of the boundary are measured (Figure 4). As shown in Figure 4, standing steel rods are used to support the wire frame at the desired height corresponding to z coordinate of the wire frame. The wire is secured to the steel rod by rubber band. In this way, boundary frames in the forms defined by (1) to (2) are realized.

Figure 5 shows the set-up used to produce soap film model. Soap film model is produced by dipping the wire-frame into a box containing soap solution with the help of a jack. The composition of the soap solution used is 25.7% of glycerin, 22.8% of concentrated car detergent and 51.5% of distilled water. The soap solution is allowed to set for one day to allow the alcohol which may exist in the detergent to evaporate. Theodolite is used to check the horizontal alignment as illustrated in Figure 6 and plan position alignment as shown in figure 10. θ in Figure 7 is for checking soap film model is in correct plan position. This is to make sure that the soap film model is suspended in such a way that the orientation of image taken using camera can be compared with mathematically defined surface.

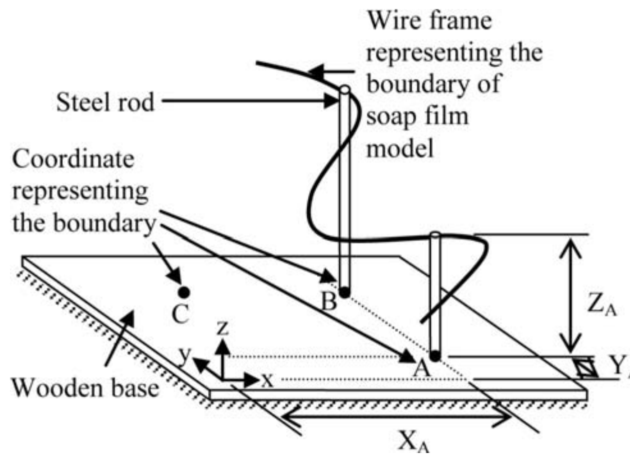

Figure 4:Making of boundary wire frame

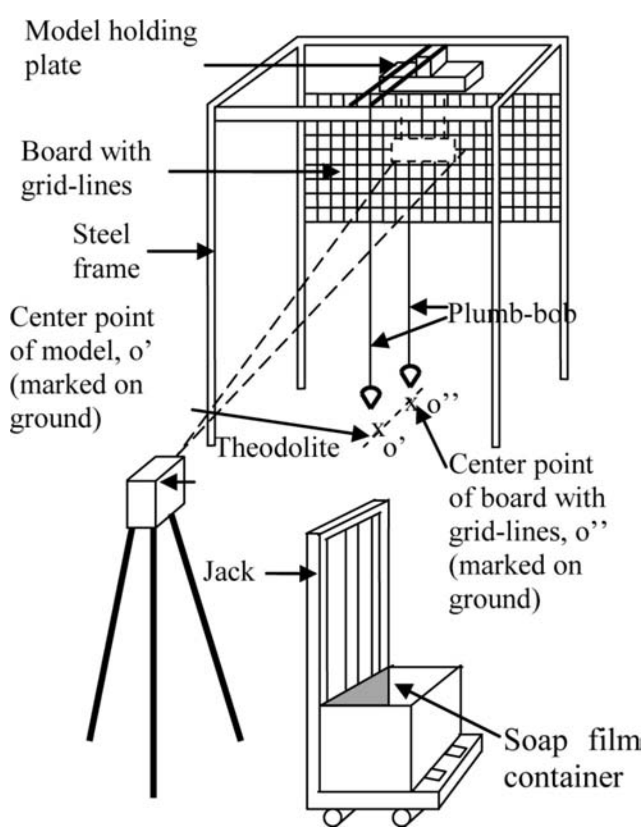

Figure 5: Set-up for the soap film model experiment

The procedures of checking of alignment of soap film model using theodolite is listed below:

(a) Plumb-bob is used to determine the projection of center point of model holding plate on the ground as shown in Figure 5. Point o' is marked on the ground.

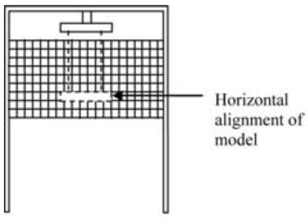

Figure 6: Horizontal alignment of the soap film model

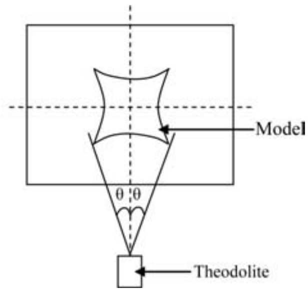

Figure 7: Plan position of the soap film model

(b) Plumb-bob is used to determine the projection of center line of board with grid-lines on the ground as shown in Figure 5. Point o'' is marked on the ground. These two points lie along a same straight line as shown in Figure 5.

(c) Theodolite is positioned at suitable distance from the frame with its view aligned along line o'-o''.

(d) Horizontal alignment of wire-frame model is checked using the theodolite.

(e) Plan alignment of wire-frame model by turning the model holding plate is checked by using the theodolite. The position of the camera is set on the place of theodolite.

After checking of proper alignment of the soap film model, the theodolite is removed. A camera is then placed at the same location as that of the theodolite to capture image of the soap film model.

4. Results of Soap Film Models

The soap film experiment set up is shown in Figure 8. In the following sections, soap film models showing good agreement with surfaces defined by (1) to (2) are first presented. This is then followed by those models where deviation has been observed.

Figure 8: Soap film experimental set up

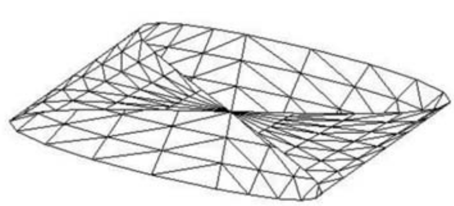

Figure 9: Mathematically defined Möbius strip (W/R=2)

4.1 Möbius strip (R/W=2)

Figure 9 shows the plan view of mathematically defined Möbius strip with R/W=2. Figure 14 shows the corresponding soap film model. Comparison of Figures 9 and 10 shows that the result obtained from soap film model is the same with mathematically defined surface which has the characteristic opening at the center.

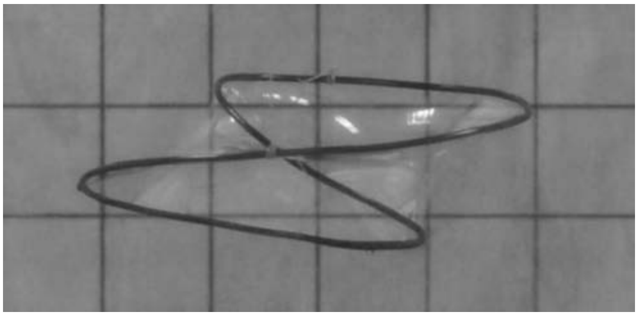

Figure 10: Möbius strip soap film model (W/R=2)

4.2 Enneper (u=v=0.86)

Figure 11 shows the mathematically defined Enneper surface with u=v=0.86. The corresponding result obtained through soap film experiment is shown in Figure 12. Comparison of the two surfaces shows that they are in good agreement.

4.3 Möbius strip (R/W=1)

Figure 13a shows the mathematically defined surface of Möbius strip with R/W=1. The corresponding Möbius strip soap film model as shown in Figure 13b does not show the characteristics of Möbius strip with opening at the center.

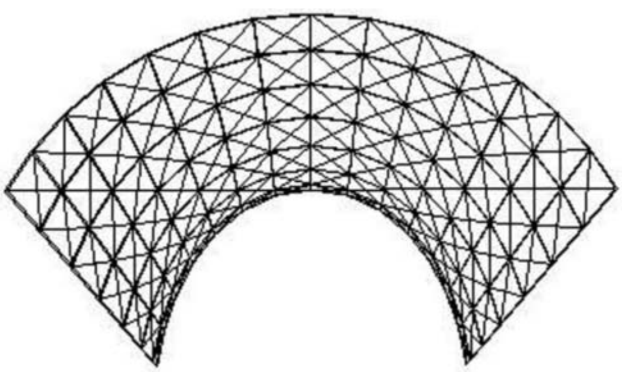

Figure 11: Mathematically defined Enneper surface (u=v=0.86)

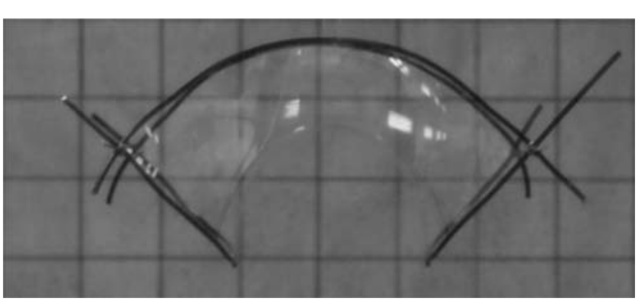

Figure 12: Enneper soap film model (u=v=0.86)

4.4 Enneper (u=v=1.25)

Enneper surface with u=v=1.25 defined by (2) is shown in Figure 14a. The corresponding soap film model is shown in Figure 14b. Comparison of Figures 14a and 14b clearly shows that the deviation of the mathematically defined Enneper minimal surface from that of soap film model.

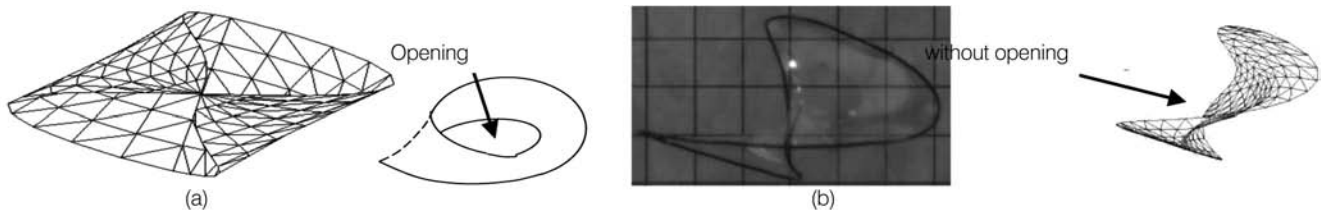

Figure 13: (a)Mathematically defined surface of Möbius strip (R/W=1) with opening at the center (b)Soap film model (Möbius strip, R/W=1)

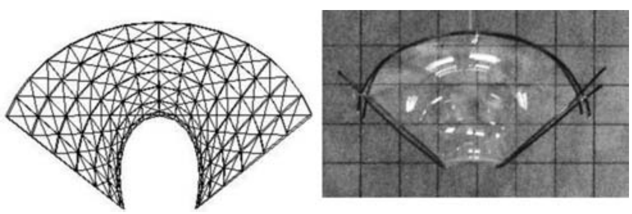

Figure 14: (a) Mathematically defined Enneper (u=v=1.25) (b) Soap film Enneper (u=v=1.25)

5. Discussion

Möbius strip surface with R/W=2, Enneper surface with parameters u=v=0.86 are found to be in good agreement with the mathematical defined surface.

For Möbius strip with R/W=2, the form obtained after soap film experiment is similar to the Möbius strip surface with opening at the center of the surface. When R/W=1, the soap film model is found to be different from the form of Möbius strip surface defined by (1). The opening of the center is missing. Such incapability of surface topology to be kept in the form of a disc under continuous changes of the boundary circle has been mentioned by [9]. This results indicates that there is a specific value of R/W ratios above which the surface of Möbius strip surface maintains the topological characteristic of disc with a central opening.

Mathematically defined Enneper surface with parameters u=v=0.86 is a stable minimal surface. The reason for the deviation of mathematically defined Enneper surface from the corresponding soap film model is probably due to the reason that for parameter u=v=1.25, Enneper surface defined by (2) no longer corresponds to stable minimal surface ([10]). Soap film model shows the corresponding stable shape under the parameter values of (u,v) = (1.25,1.25) which is different from that defined by (2).

6. Conclusion

Soap film model with surface shape in close agreement with mathematically defined Möbius strip and Enneper surfaces have been produced. Deviations between the two sets of surfaces have been shown to occur when R/W=1 in Möbius strip and parameters u=v=1.25 in the case of Enneper surfaces.

7. Acknowledgement

This research was supported by Basic Science Research Program through the National Research Foundation of Korea(NRF) funded by the Ministry of Education, Science and Technology(2011-0021548)

Author Affiliation

Hooi M. YEE[1], Kok K. CHOONG[2] and Jae-Yeol KIM[3]

[1]Faculty of Civil Engineering, Universiti Teknologi MARA, Pulau Pinang, Malaysia.

[2]School of Civil Engineering, Engineering Campus, Universiti Sains Malaysia, Pulau Pinang, Malaysia.

[3]Department of Architectural Engineering, Hyupsung University, Hwasung, Korea.

References

[1] Ireland PM., “Some curious observations of soap film contact lines”, Chemical Engineering Science, Vol. 63, 2008, pp. 2174-2187.

[2] Moulton DE, and Pelesko JA., “Theory and experiment for soap-film bridge in an electric field”, Journal of Colloid and Interface Science, Vol. 322, 2008, pp. 252-262.

[3] Brakke K.A., “Numerical solution of soap film dual problems”, Experimental Mathematics, Vol. 4, No. 4, 1995, pp. 270-287.

[4] Koiso M., and Palmer B., “On a variational problem for soap films with gravity and partially free boundary”, J. Math. Soc. Japan, Vol. 57, No. 2, 2005, pp. 334-355.

[5] Boudaoud A, Patrício P, and Amar MB., “The Helicoid versus the Catenoid: Geometrically induced Bifurcations”, Physical Reviw Letters, Vol. 83, No. 19, 1999, pp. 3836-3839.

[6] Huff R., “Soap films spanning rectangular prisms”, Geom Dedicata, Vol. 123, 2006, pp. 223-238.

[7] Weisstein and Eric W., “Möbius strip, From MathWorld—A Wolfram Web Resource”, Website: http://mathworld.wolfram.com/MoebiusStrip.html (accessed December 11 2011)

[8] Gray A., “Modern differential geometry of curves and surfaces with Mathematica”, CRC Press LLC, 1999, pp. 938-949.

[9] Caurant R., “Soap film experiments with minimal surfaces”, The American Mathematical Monthly, Vol. 47, No. 3, 1940, pp. 167-174.

[10] Nitsche and Jahannes CC., “Non-uniqueness for plateau’s problem. A bifurcation process”, Ann. Acad. Sci. Fenn. Ser. A I Math., Vol. 2, 1976, pp. 361-373.

Structural Optimization of Cable Dome Structures by using Genetic Algorithms

Byoungwook Yoon[1], Hyungmin Kim[1] and Jaehong Lee[2]

Abstract

Micro genetic algorithm is the theory of grafting the principle of survival of the fittest in genetics and it is used to solve the optimization problems. The purpose of this paper was to obtain the cross section and the optimum shape of cable dome structure by using micro genetic algorisms. The Cable dome structure was one of the tensegrity systems. The tensegrity structures are built using compressive members and tensile member. The object functions are minimum weight in all design constraints. The design constraints include stress constraints for all elements of cable dome structures, buckling constraints for struts and shape constraints for all nodes. Also, the cable dome structures are to obtain optimum shape according to initial pre-tension. This paper is shown that example problem about simple cable dome structures.

Keywords: cable domes; tensegrity structures; pre-tension; micro genetic algorithms; minimum weight design; section and shape optimization.

1. Introduction

A tensegrity structure is a pre-stress truss system involving string elements capable of transmitting loads in one direction only. Admissible connections between elements are ball joints, and external loads can be applied only at the joints. Therefore, all elements of the structure are axially loaded only, which greatly simplifies their static and dynamic modeling. This also enables the choice of materials and element geometry to be specialized for axial loads, and split further in materials optimized for compressive, and tensile stresses, and strains. However, study to optimization of tensegrity structures is incomplete. Optimization of tensegrity structures need for efficient design of tensegrity structures of sizes and shapes. So this study, optimization of four-strut tensegrity modules by using micro genetic algorithm.

2. Micro Genetic Algorithms

In the process of optimizing the structure by the genetic algorithm, if minimizing the structural weight is taken as the objective, by altering the cross section of members, the optimization may lead to optimum weight. To find an optimum design is developed to using the Micro genetic algorithms (-GA), which is proposed by Krishnakumar[5], with respect to truss structures. In the sizing and shape optimization of tensegrity, cross sectional areas and shape of geometry are considered as design variables and the coordinates of the nodes and connectivity among various members are considered to be fixed. Figure 1 shows flow chart of the micro genetic algorithm.

3. Numerical Examples

In the section, some example problems are studied for optimization by using the micro genetic algorithms. The cable domes are studied to consider as design variable of cross section and shape coordinate. Also cable domes are ap-

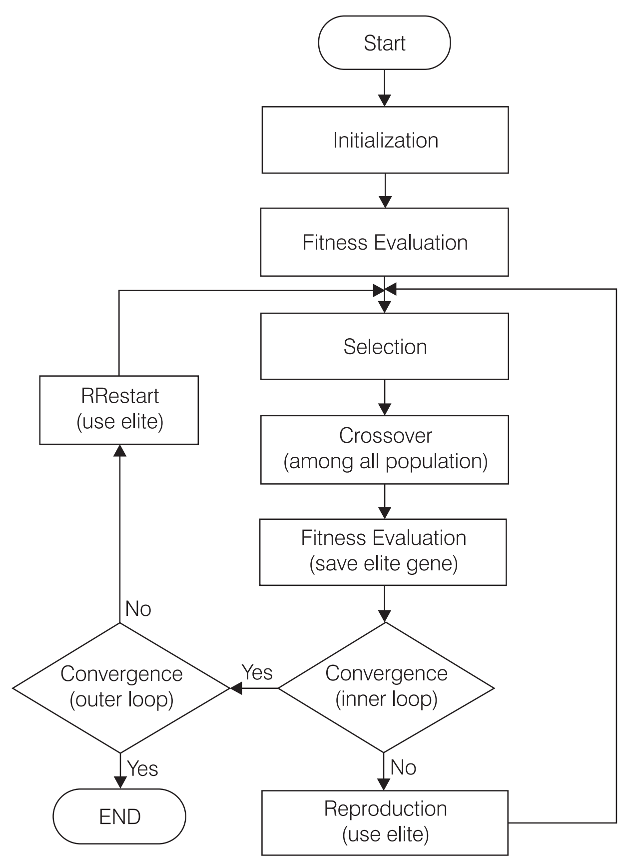

Figure 1: Micro genetic algorithm flow chart

plied to different pre-tension value. In order to minimum weight of truss structure, objective and penalty function are calculated as:

Minimize

F(X,M)=f(X)

F(X,M)=f(X)+penalty(X) (1)

$$penality(X) = r\left\{\left(\frac{\sigma(i)}{\sigma_{all}} - 1\right)^2\right\} \quad (2)$$

Where F(X,M) of Eq. 1 is value of objective function, Penalty(X) is value of penalty function. Penalty constant is defined to r at penalty function. Value of penalty function of Eq. 2 is existed to exceed allowable stress of elements, and it is increased to F(X,M) . Therefore, minimum weight of structure is resulted to minimum value of f(X) and not to existent value of penalty function.

3.1 Seven-struts Cable Dome

The Cable-dome structures in Fig. 2 illustrates the seven struts cable dome structures. This model have been proposed by some previous researcher. The seven struts cable dome structures was chosen as a base module for the numerical example. It made up of one post(center strut) and six side struts. Also, each struts are connected by cables.

All cables and struts have the material properties as Table 1. The boundary conditions were prescribed : at the six edge node was fixed in the all direction and other node boundary conditions are free. Additional loads of 100kN acts on the center node and load of 50kN acts on the side stuts. The initial force(Pre-tension) are applied as 30%, 50%

Design variables
Cross section : A1(Cables); A2(Cen-struts); A3(Side-struts) Shape : X3; Y17; Z2; Z3; Z9; Z15; Z21;
Objective functions
$f(x) = \left(\sum A_{cable} \cdot l_{cable}\right) \cdot \rho_{cable} + \left(\sum A_{strut} \cdot l_{strut}\right) \cdot \rho_{strut}$
Constraint data Stress constraints
$0 \le (\sigma_y)_{cable} \le 1670 MPa$ $\left\|(\sigma_y)_{strut}\right\| \le 235 MPa$
Material properties
Cable Young's modulus E = 2.00x10^5 MPa Density of the material ρ=7470.845kgf/m^3 Strut Young's modulus E=2.06x10^5 MPa Density of the material ρ=8759.812 kgf / m^3

Table 1: Data for design of seven-struts cable dome

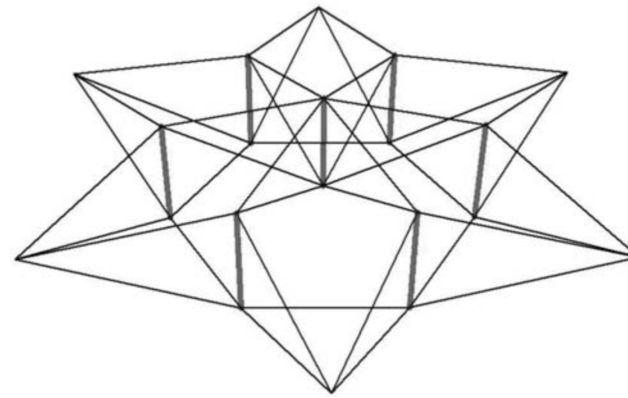

Figure 2: seven-struts cable dome

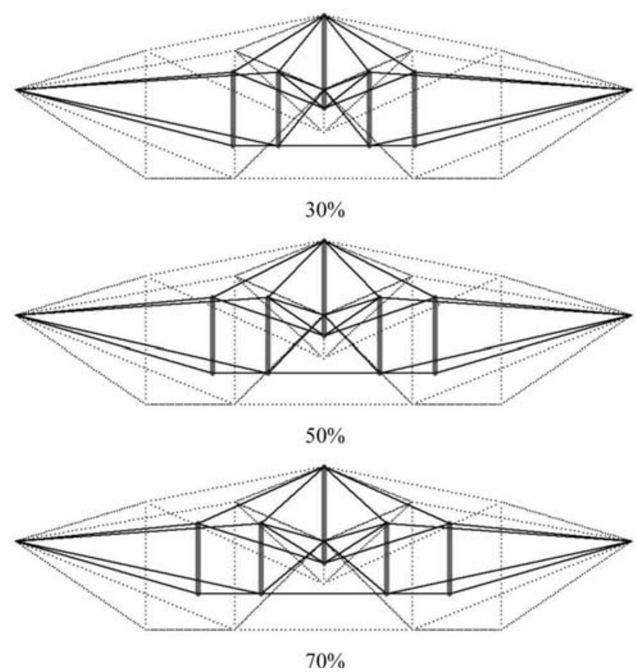

Figure 3: Shape optimal design of the seven-struts cable dome with pre-tension

and 70% of yield stress magnitude of cable. Fig. 4 show a history of optimization with respect to the seven struts cable dome structures and reliability is improved through repeated several times. It can be seen that the structural weight decreases sharply at the beginning, and decreases tardily near the optimum weight. Fig. 3 shown the optimum shape, dot lines are original shape and continuous lines are optimum shape, and obtain optimum result of seven struts cable dome structures as Table. 2

3.2 Flower Dome

The Cable-dome structures in Fig. 5 illustrates the flower dome structures. This model have been proposed by some previous researcher. The flower dome structures was chosen as a base module for the numerical example. It made up of one post(center strut) six mid-struts and six side struts. Also, each struts are connected by cables.

Shape Variable (Unit : m)		30%	50%	70%
x3		7.05	6.26	5.10
z2		-1.21	-1.15	-1.02
z3		1.00	1.00	1.00
z9		-2.95	-3.21	-3.16
Cross section (Unit : mm2)	A1(Cable)	650	330	170
	A2(Center)	53610	43370	35690
	A3(Struts)	10890	10250	5770
Weight (Unit : kgf)	Cables	2335.4	1187.0	612.5
	Struts	4805.4	4300.3	2893.1
Total Weight (Unit : kgf)		7140.8	5487.2	3505.6

Table 2: Optimal results of seven-struts cable dome

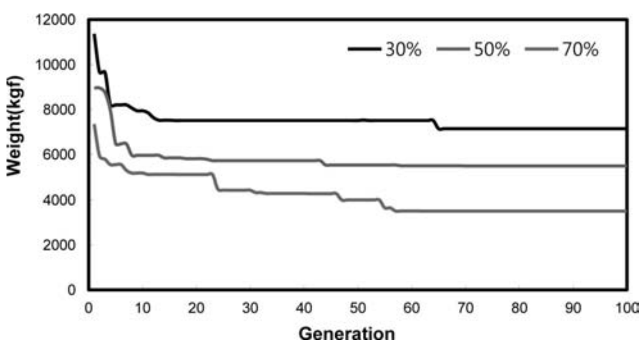

Figure 4: History of optimization with respect to the seven struts cable dome

All cables and struts have the material properties as Table 3. The boundary conditions were prescribed : at the six edge node was fixed in the all direction and other node boundary conditions are free. Additional loads of 100kN acts on the center node and load of 50kN acts on the side stuts. The initial force(Pre-tension) are applied as 30%,

Design variables

Cross section : A1(Cables); A2(Cen-struts); A3(Mid-struts) A3(Side-struts) Shape : X3; Y17; Z2; Z3; Z9; Z15; Z21;

Objective functions

$$f(x)=\left(\sum A_{cable}\cdot l_{cable}\right)\cdot\rho_{cable}+\left(\sum A_{strut}\cdot l_{strut}\right)\cdot\rho_{strut}$$

Constraint data

Stress constraints

$$0 \le \left(\sigma_y\right)_{cable} \le 1670MPa$$

$$\left|\left(\sigma_y\right)_{strut}\right| \le 235MPa$$

Material properties

Cable

Young's modulus E = 2.00×10^5 MPa

Density of the material ρ=7470.845kgf/m^3

Strut

Young's modulus E=2.06×10^5 MPa

Density of the material ρ=8759.812 kgf / m^3

Table 3: Data for design of flower dome

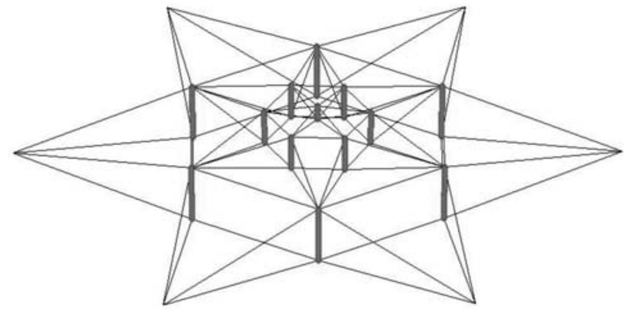

Figure 5: the flower dome

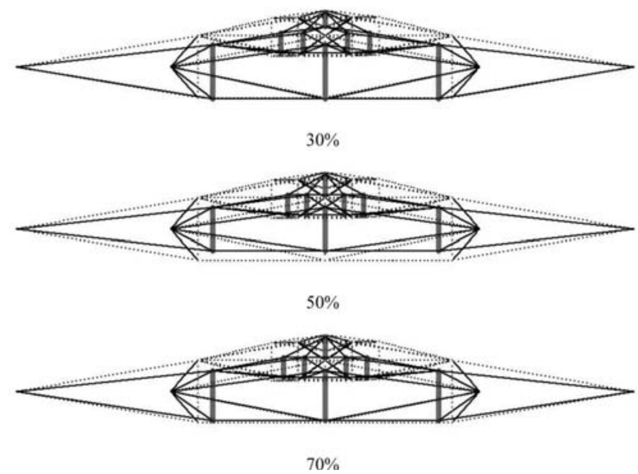

Figure 6: Shape optimal design of the flower e dome with pre-tension

Shape Variable (Unit : m)		30%	50%	70%
x3		6.51	5.51	6.06
Y17		19.01	19.00	19.03
Z2		5.93	4.98	5.03
Z3		5.00	5.00	5.00
Z9		2.05	2.04	1.98
Z15		3.26	3.17	3.07
Z21		-4.64	-3.12	-4.21
Cross section (Unit : mm^2)	A1(Cable)	660	1700	1700
	A2(Cen-struts)	4970	24200	3300
	A3(Mid-Struts)	3230	6500	7300
	A4(Side-Struts)	23000	18000	24000
Weight (Unit : kgf)	Cables	6388.3	16424.3	16446.4
	Struts	10098.4	7539.1	10470.4
Total Weight (Unit : kgf)		16486.7	23963.3	26916.8

Table 4: Optimal results of flower dome

50% and 70% of yield stress magnitude of cable.

Fig. 7 show a history of optimization with respect to the seven struts cable dome structures and reliability is improved through repeated several times. It can be seen that the structural weight decreases sharply at the beginning, and decreases tardily near the optimum weight. Fig. 6

shown the optimum shape, dot lines are original shape and continuous lines are optimum shape, and obtain optimum result of seven struts cable dome structures as Table. 4

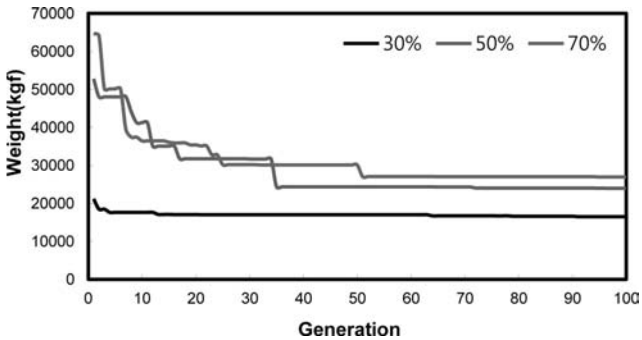

Figure 7: History of optimization with respect to the flower dome

4. Conclusions

This study is developed optimum design of cable dome structures by using micro genetic algorithms(μ-GA) which is optimization technique. Micro genetic algorithm has a merit not to need mathematics knowledge for optimum design of structures, and it can be applied to analysis program of structure. Features of the proposed method, cable dome structures are demonstrated by solving a problem. From the example of cable dome structures, micro genetic algorithm is found the optimum shape and cross section. The cable domes obtained different optimal design by pretension. Therefore, the cable domes have optimal pre-tensions for minimum weight.

5. Acknowledgement

This research was supported by Basic Research Laboratory Program of the National Research Foundation of Korea (NRF) funded by the Ministry of Education, Science and Technology through NRF2011-0027949.

Author Affiliation

Byoungwook Yoon[1], Hyungmin Kim[1] and Jaehong Lee[2]

[1]Department of Architectural Eng., Sejong University, Seoul, Republic of Korea.

[2]Department of Architectural Eng., Sejong University, Seoul, Republic of Korea,

6. References

[1] Goldberg D.E, Sizing Populations for Serial and Parallel Genetic Algorithms, Proceeding 3rd International Conference on Genetic Algorithms and Their Application, Arlington, VA, pp.70-79, 1989.

[2] Goldberg D.E, Genetic Algorithms in search, Optimization and machine Learning, Addison-Wesley, 1989.

[3] Jenkins W.M, Structural Optimization with the Genetic Algorithm, The Structural Engineer, Vol. 69. No.24, pp.419-422, 1991.

[4] Kaveh A and Kalatjari V, Size/geometry Optimization of Trusses by The Force Method and Genetic Algorithm, ZAMM-Journal of Allpied Mathematics and Mechanics, Vol. 84, No.5, pp.347-357, 2004.

[5] Krishnakumar K, Micro-genetic Algorithm for Stationary and Non-stationary Function Optimization, SPIE, Intelligent Control and Adaptive Systems, Vol.11, No.96, pp.282-296, 1989

Seismic Response of Single Layer Latticed Cylindrical Shell Structures with Seismic Isolation System

Yukihiro Matsumoto[1], Seishi Yamada[2], Kenji Sasahara[3] and Takeshi Seino[3]

Summary

In this paper, it has been analysed that fundamental seismic response behaviour using the finite element analyses, and shown the effects of rigidity of the roof structure and sub-structure on the various response quantities. Then, the isolation system having angle has adopted in sub-structure to reduce the seismic response. Based on these, it is confirmed that the seismic isolation system in sub-structure effectively reduce the seismic vibration on horizontal earthquake input. It has been suggested that the present seismic isolation system would provide a safe, simple and realistic seismic design for single layer latticed cylindrical shell structures.

Keywords:

Single layer latticed cylindrical shell; seismic response; seismic isolation system.

1. Introduction

For the design of shell-like space frames located in seismic area, it is very important to give considerable attention to the seismic response behaviour and to make clear how to reduce the seismic response. However, for single layer latticed cylindrical shell structures, it has not been enough to make clear their dynamic responses and to reduce the seismic responses during earthquake. The authors have previously carried out the seismic response analyses and discussed on the fundamental seismic response behaviour of this kind of structures using finite element method. Then, an alternative static load modelling procedure associated with the dynamic vibration analytical results has then been proposed. It is very considerable characteristic that the distribution functions of the previously proposed static seismic loading model associated with the dynamic vibration analytical results are corresponding to the displacement functions for simple supported shallow shell. Based on these, the orthotropic continuum shell analogy has been applied to the latticed cylindrical shell roof to simplify the estimation of the seismic response. Then an alternative static load modelling procedure has been proposed using the continuum shell analogy [1, 2].

Based on these backgrounds, in this paper, the effects of rigidity of the roof structure and sub-structure on the various response quantities have examined using the finite element method. And the applicability of the seismic isolation system for single layer latticed cylindrical shell structures has investigated. Then, the effects of seismic isolation system on the seismic responses quantity are discussed in detail.

2. Analytical Models

2.1 Structural Models

Figure 1 shows the analytical models and Table 1 the geometric condition of the analytical models. The analytical models were adopted to be single layer latticed cylindrical shell structures, having open angle ϕ, radius of curvature R, length of longitudinal direction LX, length of span direction LY. All members are to be straight circular steel tubes with Young's modulus E $=$205GPa and Poisson's ratio ν $=$0.3.The joints are assumed to be rigid. The adopted analytical parameters are of the horizontal resistance of the substructure. The substructures are designed by using

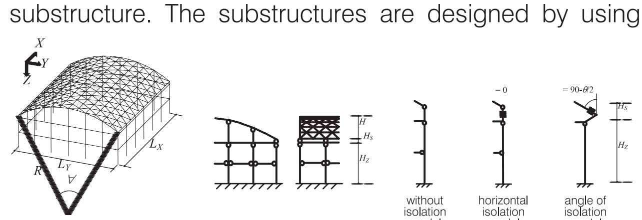

Figure 1: Analytical models

	LY [m]	LX [m]	H [m]	R [m]	ϕ [deg]	HS [m]	HZ [m]
G121245			2.33	30.57	45		
G121260	23.40	24.40	3.14	23.40	60	0.5	6.0
G121275			3.97	19.22	75		

Table 1: Geometric condition of the analytical models

of the base shear coefficient, 0.2, and the displacement of top of column, δ, are controlled to be HZ/200 (S02), HZ/400 (S04), HZ/500 (S05) and HZ/1000 (S10) millimeter. The adopted boundary condition is fixed support at the bottom of columns. The member section of shell roof of analytical models is shown in Table 2.

	M1	M2	M3	M4
Diameter [mm]	101.6	114.3	139.8	165.2
Thickness [mm]	3.2	4.5	4.5	4.5
Sectional area[mm2]	989.2	1552	1913	2272
Geometrical moment of inertia [cm4]	120	234	438	733

Table 2: Member condition of the analytical models

2.2 Structural Isolation System

In this study, the seismic response behaviour of the single layer latticed cylindrical shell structures with seismic isolation in the substructure is analysed. The rigidity of seismic isolation system is designed by using of the natural period and the natural period is controlled to be 2.0 (F20), 1.5

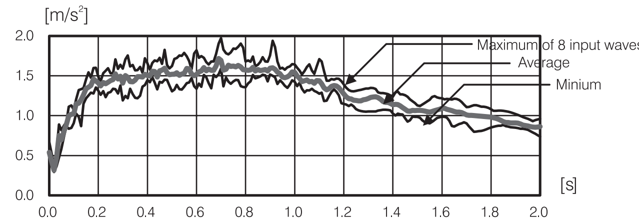

Figure 2: Acceleration spectra of adopted input waves

(F15) and 1.0Hz (F10) as following equation.

$$k = \frac{4\pi^2 f^2 w}{g} \qquad (1)$$

where, W is the total weight of roof structure, g gravity acceleration. The analytical models having seismic isolation system are adopted to be "horizontal isolation model" and "normal isolation model" as shown in figure 1.

2.3 Input Waves

The input waves are the artificial earthquake waves hav-

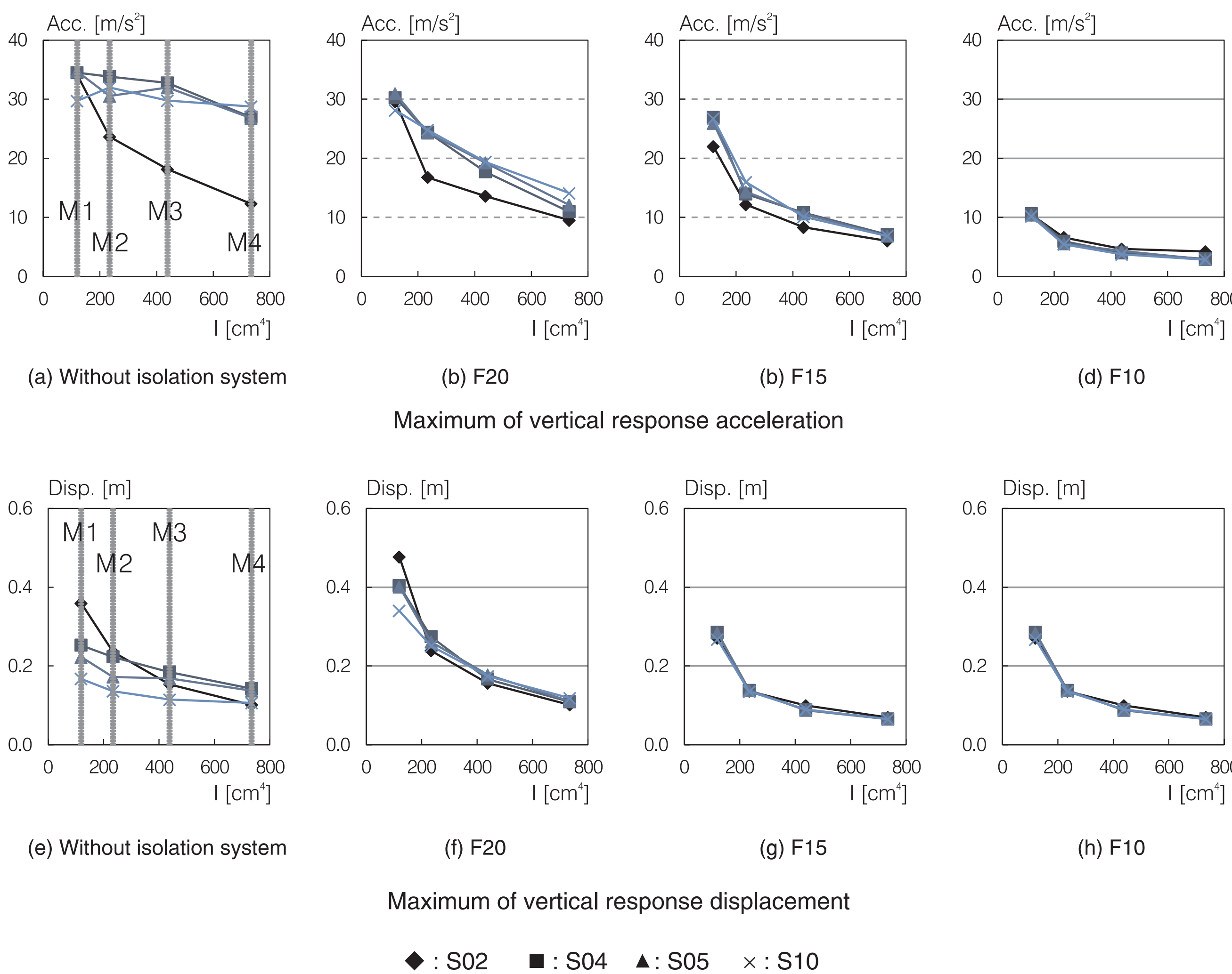

Figure 3: Maximum of vertical responses

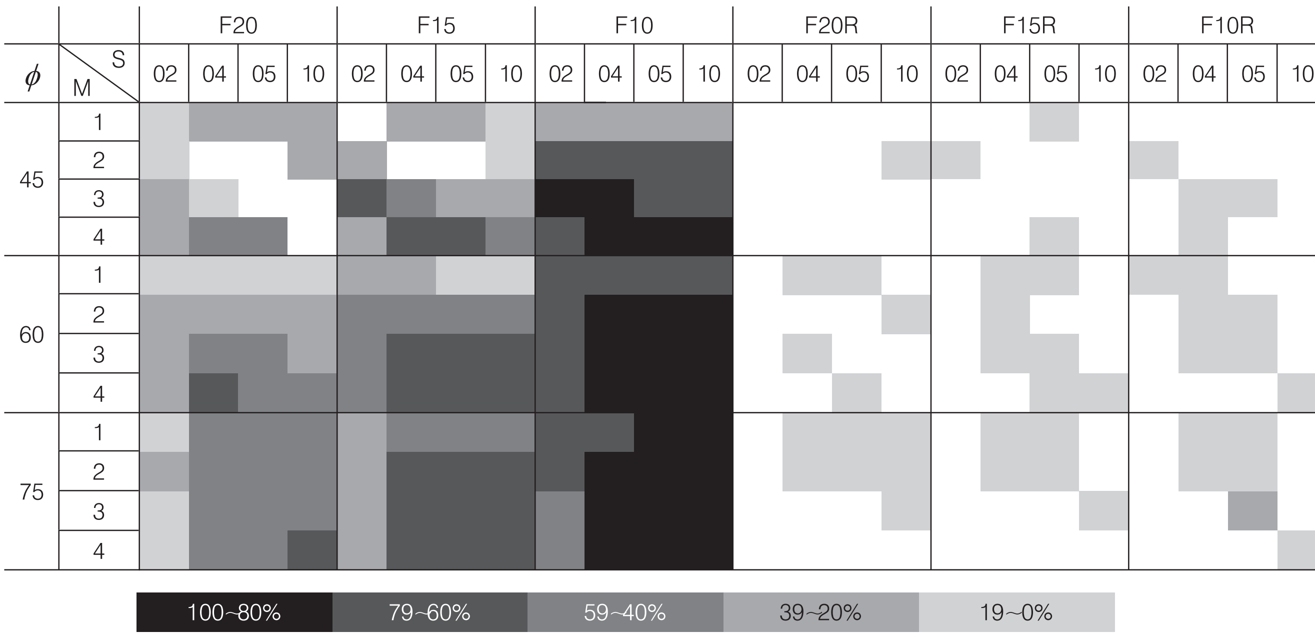

Table 3: Decrease ratio of vertical response accelerations

ing the various phase characteristics and target spectra. The input horizontal earthquake waves are based on the design acceleration response spectrum of the safety limit level given in the Notification 1457 of the design regulation from the Ministry of Land Infrastructure and Transport of Japan. The soil condition adopted to be the kind II also given in the Notification 1457 of the design regulation of Japan. The damping ratio, h, in the structure assumed to be 0.02. Figure 2 shows the acceleration spectra of artificial earthquake. The phases of input waves are based on El Centro-NS, EW (1940), Taft-NS, EW (1952), Hachinohe-NS, EW (1968) and Kobe-NS, EW (1995).

3. Results of Dynamic Response Analysis

Figure 3 shows the results of seismic response analysis. The vertical axis is the maximum of vertical response acceleration and the horizontal axis the geometrical moment of inertia of roof members. In the case of S02, as stiffness of roof member become higher, the maximum value of vertical response acceleration decreases as shown in figure 3 (a). Because the roof structure vibrates as the rigid body and the substructure influences the roof structure like the seismic isolation structure. Also as stiffness of roof member become higher, the maximum value of vertical response displacement decreases in all analytical model as shown in figure 3 (b). In the case of S02, S05 and S10, the decrease ratio of the vertical response is smaller than the increase ratio of the axial and bending stiffness of roof members. In the case of maximum of vertical response acceleration, the isolation system effectively decreases the seismic response as shown in figure 3 (b), (c) and (d). However, in the case of maximum of vertical response displacement, the amount of decrement of seismic response depend on the stiffness of roof members; as stiffness of roof member become higher, the maximum value of vertical response displacement decreases because the vibrational mode change to the swaying mode as shown in figure 3 (f), (g) and (h). Table 3 shows the decrease ratio of vertical response accelerations. The advantageous effect of horizontal seismic isolation system is observed in almost all analytical models. However, in the case of the normal seismic isolation system, the effect of isolation system is not observed in many analytical models. Also in the case of the horizontal seismic isolation system, the large horizontal deformation is predicted caused by thrust force under sustained loading. Therefore, the angle of seismic isolation system is investigated as shown in figure 4. The left vertical axis is the decrease ratio of vertical response acceleration, the right vertical axis the horizontal deformation caused under sustained loading, the horizontal axis the angle of isolation system, θ. In the case of ϕ=60degree, the horizontal displacement of isolation system is decreased by about 50% compared with the horizontal isolation by the angle of isolation system, θ, is changed to 30degree. And the maximum of vertical response acceleration is decreased by 24% (F15) or 35% (F10). Also in the case of ϕ=75degree and ϕ=35.6degree, the horizontal displacement of isolation system is decreased to 0 and the maximum of vertical response acceleration is decreased by 32% (F15) or 35% (F10). Figure 6 means that both horizontal displacement and maximum of vertical response can be decreased to adopt the suitable angle of the isolation system.

4. Conclusions

In this paper, the seismic response behaviour of single layer latticed cylindrical shell structure with seismic isolation system was shown. And the effects of angle of seismic

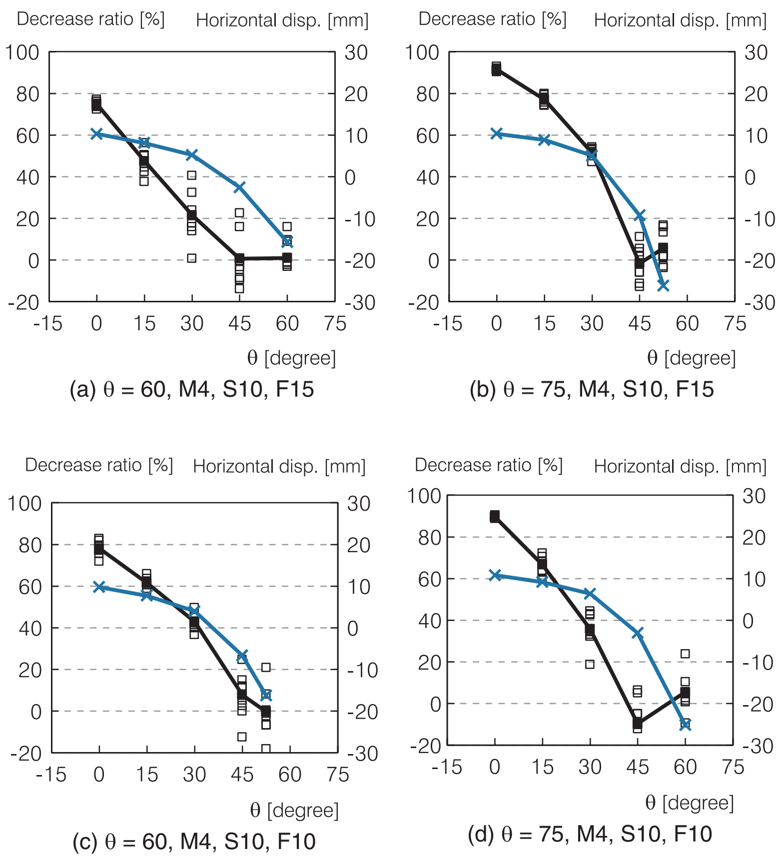

(a) θ = 60, M4, S10, F15

(b) θ = 75, M4, S10, F15

(c) θ = 60, M4, S10, F10

(d) θ = 75, M4, S10, F10

■ : Average of decrease ratio

□ : Decrease ratio obtained by dynamic response analysis

× : Horizontal displacement of isolation system

Figure 4: Effect of the angle of the isolation system

isolation system on seismic response were investigated in detail. The remarkable effect of seismic isolation system was made clear in almost all analytical models. And it was proposed that both horizontal displacement and maximum of vertical response can be decreased to adopt the suitable angle of the isolation system. Furthermore, it was suggested that the suitable angle of the isolation system, θ, is to be between 0 and 90 - ϕ /2degree.

Author Affiliation

Yukihiro Matsumoto[1], Seishi Yamada[2], Kenji Sasahara[3] and Takeshi Seino[3]

[1] Assistant Prof., Department of Architecture and Civil Eng., Toyohashi University of Technology, Toyohashi, Japan

[2]Prof., Department of Architecture and Civil Eng., Toyohashi University of Technology, Toyohashi, Japan

[3]Graduate Student, Department of Architecture and Civil Eng., Toyohashi University of Technology, Toyohashi, Japan

References

[1] Seishi Yamada, Yukihiro Matsumoto and Eiji Saito, "Static seismic load modeling using continuum shell analogy for single layer latticed cylindrical shell structures", CD-ROM Proceeding of International Symposium on Shell and Spatial Structures, 2006.

[2] Yukihiro MATSUMOTO, Seishi YAMADA, Sho SAITO and Takashi TAGUCHI, "Effects of hysteresis dampers in framed substructures on the responses of steel latticed cylindrical shell roofs", Proceeding of The 9th Asian Pacific Conference on Shell and Spatial Structures, 2009.

[3] Shiro Kato, Shoji Nakazawa, Fujio Matsushita, Takanori Ohya,Tetsumi Okamoto, "A new system of intermediate isolation for space structures against earthquakes, Spase Structures 5 Thomas Telford, Fifth International conference on Space Structures, pp.1053-1062, 2002.

[4] Shiro Kato, Shoji Nakazawa, Mizuaki Uchikosi, Yoichi Mukaiyama, "Response reducing effect of seismic isolation system installed between large dome and lower structure", Proc. of Sixth Asian Pacific Conference on Shell and Spatial Structures, pp.323-330, 2000.

Soil Improvement Using Vibro Replacement Technique

[1]Ali Dadashzadeh Sayar, [1]Mohamadhasan Khalilpasha

Abtract

If the properties of the existing soil cannot fulfill the requirements set by the proposed loading conditions, bearing capacity, lateral stability and earthquake induced liquefaction potential, various techniques propose an economical solution for the ground improvement. Soil improvement methods should be determined only after development and analysis of the complete geotechnical record. This record includes groundwater depth, subsoil stratification, soil strength and type, consolidation and compaction characteristics, permeability, liquefaction strength, and dynamic deformation characteristics. Additional testing for bearing capacity or slope stability may also be required for determination of appropriate remediation techniques. As there are many soil improvement techniques and minor variations often occur in the industry; therefore, it is important to work closely with the contractor to fully understand the effect or influence of each variation. In this paper, popular techniques, Deep Vibro Techniques especially Vibro Stone Columns will be explained. Finally the case study having done in the north of Iran is described.

Introduction

The ground improvement techniques being used today have significantly shortened the timeframe for preparing the new land for use and therefore secured the economic viability of many projects. The consolidation phase has become an essential part of soil improvement and several techniques have been developed to stabilize the new ground

The main goal of most soil improvement techniques used for reducing liquefaction hazards is to avoid large increases in pore water pressure during earthquake shaking. This can be achieved by densification of the soil and/or improvement of its drainage capacity. Soil improvement is also applied to improve the mechanical characteristics of impure soft soil.

When building on many sites with poor ground conditions the most economical approach to the foundations is to improve the bearing pressure rather than attempt to bypass the weaker soils with piled foundations. Ground Improvement systems can typically be 50% of the costs of a piling scheme but, more importantly, further cost benefits are provided by adopting simpler sub structures and in most cases the lack of spoil generation.

Vibro Flotation is a collective term for forms of ground improvement brought about by inserting a vibrating poker into the ground, and includes Vibro Compaction and Vibro Replacement. The latter process is often referred to as Vibro Stone Columns. The Vibro Compaction Technique compacts granular soils with negligible fines content by rearrangement of the soil particles into a denser state.

The Vibro Replacement Technique builds load bearing columns made from gravel or crushed stone in cohesive soils and granular soils with high fines content (Figure 1).

For all techniques the Vibro process starts with the penetration of the oscillating vibrator into the ground to the required improvement depth. The soil treatment is carried out on extraction by either compacting the soil or by building a stone column or structural element from the bottom up.

The deep Vibro Techniques provide a highly versatile ground improvement method that can be adjusted to a wide variety of ground conditions and foundation requirements. Its execution is comparatively fast even if large volumes of soil are to be improved and subsequent structural works can follow quickly. The soil improvement enables the contractor to utilize standard shallow footings or ground bearing slabs which, in turn, leads to additional savings compared to suspended floor options. Another advantage is its en-

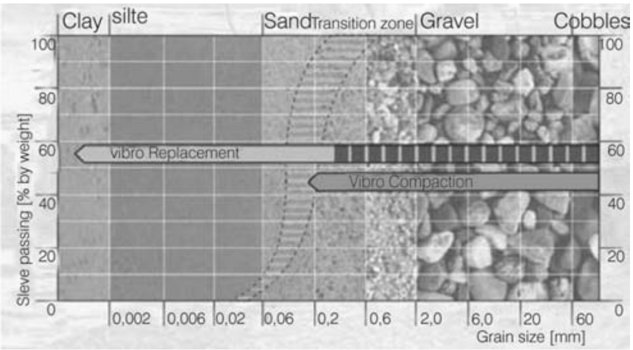

Fig. 1: Particle size distribution illustrating applicability of Vibro-Compaction and Vibro-Replacement.

vironmental friendliness of the deep Vibro Techniques, as natural and in situ materials are used and a comparatively small quantity of soil is removed in the process.

Vibro Replacement Columns

Cohesive, mixed, and layered soils generally do not densify easily when subjected to vibration alone. Vibro Replacement extends the range of soil types that can be improved with a deep vibratory process. Vibro Replacement is similar to Vibro Compaction except that rather than sand; a gravel backfill is used, with the columns providing both a minimal degree of reinforcement to the soil and an effective means of additional drainage. Vibro Replacement is appropriate for soft, cohesive soils, and with saturated soils having fines greater than 12%.

The Vibro Replacement method is also used in granular soils with high fines contents and in cohesive soils. For the construction of Vibro Replacement columns the bottom or top feed processes can be employed to optimize the performance of this process and to accommodate the specialized equipment, the Vibrocat base unit has been developed which guides the vibrator on its leader and allows the exertion of an additional pull- down pressure during penetration and compaction.

The Vibro Replacement process consists of alternating steps. During the retraction step, gravel runs from the vibrator tip into the annular space created and is then compacted and pressed into the surrounding soil during the following re-penetration step. In this manner stone columns are created from the bottom up, which act as a composite with the surrounding soil under load (Figure 2).

The Vibro Replacement process, does not assume any compaction in the surrounding soil. The improvement relies on the higher stiffness and higher shear strength of the stone column. While the compaction of the surrounding soil can be easily verified by surroundings, the improvement effect of the Vibro Replacement can best be checked by in situ load tests.

The effectiveness of Vibro Replacement depends to a large extent on the soil type, column installation technique, relative spacing of columns and column diameter. During installation, the uncased Vibroflot penetrates to the desired depth, stone is added, and the vibroflot is plunged until the desired level of compaction is obtained. Typical columns vary from 30 to 42 inches in diameter, with depths to 100 feet. Stone columns greatly increase bearing capacity, settlement properties, and shear strength of soft clay soils. The critical depth for effectiveness with respect to increased bearing capacity is typically four column diameters.

For the foundation design, the improved ground is treated as normal subsoil. The allowable bearing pressure that is achieved after the improvement is typically in the range of 150 to 400 kPa. Mixed grained and fine grained soils frequently do not possess a sufficient bearing capacity. For fines content in excess of 10% to 15% the soils cannot be effectively compacted without the introduction of additional material. For these cases the Vibro Replacement Technique is a viable option. This technique is also suitable for the treatment of coarse fills such as rubble, building debris and slag heaps.

Case Study

Case study is about three oil tanks of 150 thousand barrel, located in the town of Neka (northern of Iran); will be constructed to increase the storage capacity of imported oil.

Based on geotechnical investigation, having done by Irankhak consulting engineering company in 2008, because of high groundwater table and existing sandy soil with medium dense (resulting from SPT test), liquefaction risk of soil underneath the oil tanks to upper 15 meter depth is definite during earthquake. In the other hand, according to the mechanical parameters of soil around the case, obtained from the result of in-site and laboratory test, bearing capacity will not be satisfied. So it is needed to solve these two problems by improving the soil underneath the oil tank. Based on Geotechnical studies and compared the cost and the time of the soil improvement methods, the correct selected option was Vibro Replacement Columns. Because of different methods to execute Vibro Replacement Columns the use of contractors experienced in the use of this method lies in the strict recommendations.

Understanding the underground layers, based on field studies of a borehole drilled (depth 30 m) from the geotechnical studies have been done. The soil profile is divided into three layers as follows:

- First layer: This layer of the surface to a depth of 4 classified to poorly sandy soil (SP) with layers of sand with silt (SM), from the results of the standard penetration test lies in the dense class.
- Second layer: This layer depth of 4 to 16.5 m from the classified to fine clay and silt (CL, CL-ML) with layers of sand with clay and silt (SM ,SC).
- The third layer: including the depth of 16.5 m to the end of the drilling depth consists of the alluvial sand with clay and sand with silt (SM, SC) lies in the medium density class.

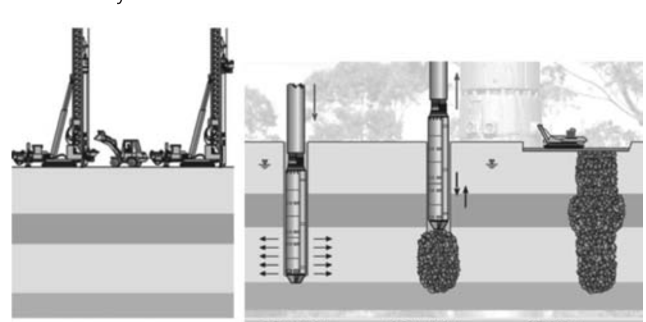

Fig. 2: Process of Vibro Replacement.

Groundwater level in the project is located at a depth of 2 m from the surface. In Figure 3 the execution phases of the Drilling and arm vibration in the sand columns are shown. During constructing stone columns with Vibro Replacement, 15 to 35 percent of poor soil volume is replaced with suitable dense materials. Diameter of stone columns is about 70 to 120 cm. The effective radius of this type of soil improvement, that is functions of grain size and the amount of incoming vibration energy and the fine grained percent, is normally about 0.60 to 1.5 meter (from the column center). Therefore it is necessary to act in a regular grid with distances of about 1.5 to 3.5 m in whole.

To select the grain size it is necessary to consider parameters such as shear strength, ability of vibration compressibility and capability of proper drainage. Before executing Vibro Replacement Columns, to ensure the accuracy of the execution and designing method and to determine optimum distance between columns, three experimental patterns are run.What will change in these patterns is the distance of the grid points, which is equal to 1.6, 1.8 and 2 m that is considered in the triangular form. However, the company proposed to eliminate the pattern of 1.6 m (due to difficulty of executing columns in the form of triangular at intervals of less than 1.8 m) and adding a test pattern 2.2 meter. Finally it is observed that the distance of 1.6 meter is away from the optimal minimum distance and the distance of 2 m does not provide the desired density at all depth. Thus pattern of 1.8 meter provides better alignment with considering operational projects and technical issues.

Conclusion

Reviewing many trials and tests, the conclusion must be drawn that many options exist which can successfully accelerate the consolidation of soils to develop newly reclaimed land or compaction methods to stabilize subsoil in vulnerable seismic areas. Each technique has its own advantages and disadvantages in relation to time, cost and performance. The best method is always to consider the specific needs of a project and contact specialist contractors to evaluate the needs of the project.

The conclusions are as following

1. The Deep Vibro Techniques provide a highly adaptable ground improvement method that can be adjusted to a wide variety of ground conditions and foundation requirements. Its execution is comparatively fast even if large volumes of soil are to be improved and subsequent structural works can follow quickly.
2. The Vibro Replacement method is used in granular soils with high fines contents and in cohesive soils.
3. The Vibro Stone Column technique is one of the most widely-used ground improvement processes in the world. Historically the system has been used to densify loose granular soils, but over the past 35 years, the system has been used increasingly to reinforce soft cohesive soils and mixed fills.
4. Vibro Replacement is also appropriate for soft, cohesive soils, and with saturated soils having fines greater than 12%.
5. The stone column is possibly the most "natural" foundation system in existence. Stone columns consist entirely of gravel, a substance that is found naturally in the subsoil. No additives are mixed into the stone columns. They are therefore not only environmentally neutral but also more durable than any other foundation system that would involve the use of cement or steel.
6. Based on Geotechnical studies in Neka (northern of Iran) and compared the cost and the time of the soil improvement methods, the correct selected option was Vibro Replacement Columns. Because of different methods to execute Vibro Replacement Columns the use of contractors experienced in the use of this method lies in the strict recommendations.

Author Affiliation

[1]Ali Dadashzadeh Sayar, [1]Mohamadhasan Khalilpasha

[1]Dept. of Civil Engineering, Islamic Azad University, Jouybar, Iran.

Reference

- Barbara, S., P.E. Moffat, "Soil Remediation Techniques for Reduction of Earthquake Induced Liquefaction ",Senior Structural Engineer, Jacobs Civil Inc.,
- Kramer, Steven L., 1996. "Geotechnical Earthquake Engineering", Pub I. Prentice Hall.
- Andrus, Ronald D. and Chung, M. Riley, 1995. "Ground Improvement Techniques for liquefaction Remediation near Existing Lifelines." National Institute of Standards and Technology,

Soil Improvement Using Vibro Replacement Technique

- Mitchell, J.K., 1981. "Soil Improvement" – State of the Art Report, Proc. 10th ICSMFE. Vol. 4.
- McKelvey, D., V. Sivakumar, A. Bell and J. Graham, 2004. " Modeling vibrated stone columns in soft clay", Proceedings of the Institute of Civil Engineers Geotechnical Engineering, 157: 137-149.
- Priebe, H.J., 1995. "The design of Vibro Replacement", Ground Engineering (Dec), pp: 31-37.
- Raju, V.R., R. Hari Krishna and R. Wegner, 2004. "Ground improvement using Vibro Replacement in Asia 1994 to 2004 - a 10 year review", Proceedings of 5th Int. Conf. on Ground
- Sondermann, W. and W. Wehr, 2004. "Deep Vibro Techniques, Ground Improvement", 2nd Edition, edited by M.P. Moseley and K. Kirsch, pp: 57-92, Spon Press.
- Wehr, J. and I. Herle, 2006. "Exercise on calculation of stone columns", Pribe method and FEM, Proceedings of the 6th European Conference on Numerical Methods in Geotechnical Engineering, Graz, pp: 773-776.
- Information on http://www.kellerge.com.au
- Information on http://www.vibroflotation.com/

Technical Characteristics of Friction Pendulum™ Bearings

Victor Zayas

General Description

Friction PendulumTM bearings are seismic isolators that are installed between a structure and its foundation to protect it from damage due to earthquake shaking. The bearings reduce lateral loads and shaking movements transmitted to the structure. They can protect structures and their contents during strong, magnitude 8 earthquakes, and can accommodate near fault pulses and deep soil sites.

Friction PendulumTM bearings use the characteristics of a pendulum to lengthen the natural period of the isolated structure so as to avoid the strongest earthquake forces. The period of the bearing is selected simply by choosing the radius of curvature of the concave surface. It is independent of the mass of the supported structure. Torsion motions of the structure are minimized because the center of stiffness of the bearings automatically coincides with the center of mass of the supported structure.

The bearings offer versatile properties which can satisfy the diverse requirements of buildings, bridges and industrial facilities. The bearing's period, vertical load capacity, damping, displacement capacity, and tension capacity, can all be selected independently. Dynamic periods from 1 to 5 seconds, and displacement capacities of up to 60 inches can be provided. Dynamic frictions from 3% to 20% are available. Effective damping ranges from 10 to 40%. Individual bearings can support vertical loads up to 30 million pounds, and tension load capacities of up to 2 million pounds. The Friction PendulumTM bearing's versatile properties permit the seismic isolation design to be optimized for best seismic performance and lowest construction cost. The reliability of the dynamic and sliding properties of Friction PendulumTM bearings has been verified through hundreds of rigorous tests performed at internationally renowned earthquake engineering research centers [Refs. 1, 4, 6, 7, 9, 15, 16, 17, 18, 27, 28, 29, 30]. Test results demonstrate a consistent and reliable bi-linear response with no degradation under repeated cyclic loadings. The specified effective stiffness and damping values are accurately delivered for either unscragged or scragged bearings, new or aged bearings, and for temperatures ranging from 30 °F to 100 °F. Tests of full-size bearings show that they retain their full strength and stability throughout their displacement range, with high strength factors of safety.

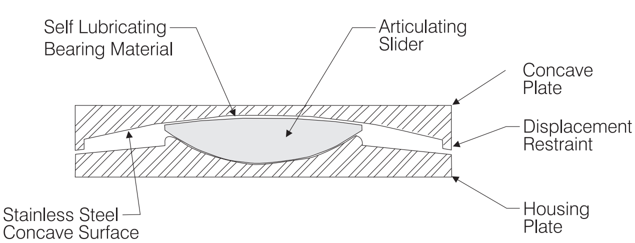

Bearing Section

Dynamic Properties

Friction PendulumTM seismic isolation bearings are based on an innovative way of achieving a pendulum motion. Geometry and gravity achieve the desired seismic isolation properties. The result is a simple and stable seismic response. The isolator period is controlled by the selection of the radius of curvature, R, of the concave surface. The natural period of vibration of a rigid structure supported on Friction PendulumTM bearings is determined from the pendulum equation,

$$T = 2\pi\sqrt{(R/g)}$$

where g is the acceleration of gravity.

When the earthquake forces are below the friction force level, a Friction PendulumTM supported structure responds like a conventionally supported structure, at its non-isolated period of vibration. Once the friction force level is exceeded, the structure responds at its isolated period, with the dynamic response and damping controlled by the bearing properties.

The operation of the bearing is the same whether the concave surface is facing up or down.

The Friction PendulumTM bearing has the flexibility to achieve a wide range of properties. Changing the sliding period from 2 to 3 sec. reduces the base shear and increases the displacement. Changing the friction coefficient from 0.10 to 0.05 further reduces the base shear and increases the displacement.

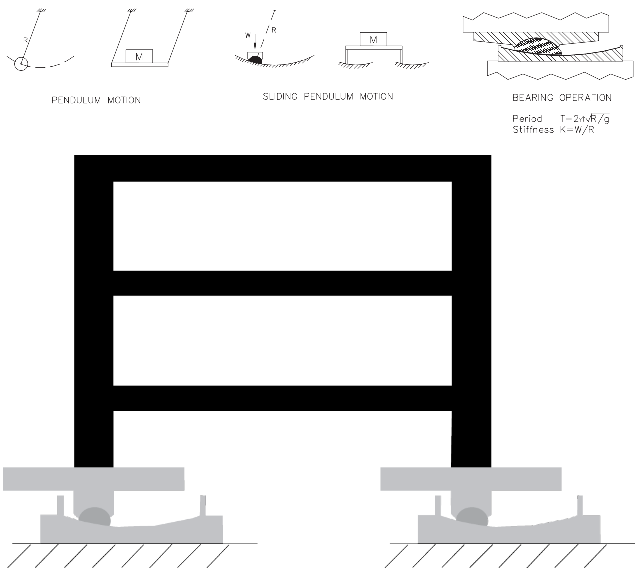

Principles of Friction Pendulum Bearing Operation

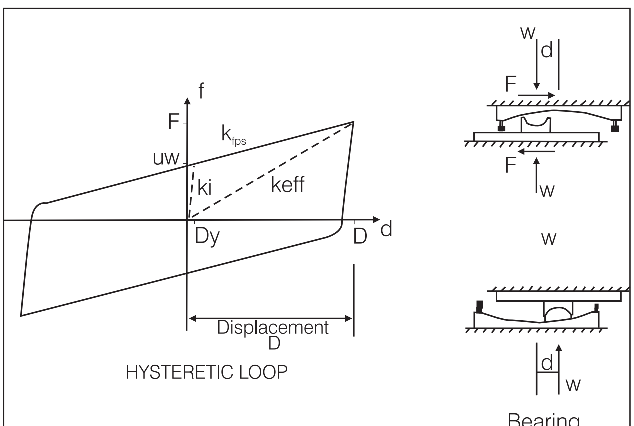

Definitions

U = Dynamic Friction
W = Vertical Load
R = Radius of Curvature
Ki = Initial Stiffness = $\frac{uW}{Dy}$
Kfps = Stiffness of FP Bearing = $\frac{W}{R}$

D = Design Displacement
$F = uW + \left[\frac{W}{R}\right]D$
T = Bearing period = $2\pi\sqrt{\frac{R}{g}}$
Keff = Effective Stiffness = $\frac{F}{D}$
Teff = Effective Period = $2\pi\sqrt{\frac{W}{keff*g}}$
B = Effective Damping = $\left[\frac{u}{u+D/R}\right]$
Dy = 0.10 in

The semi-spherical design of the articulated slider achieves relatively uniform pressures under the articulated slider. The relatively uniform pressure distribution reduces slip-stick motion and prevents high local bearing pressure from occurring. The lateral restoring stiffness of the Friction PendulumTM bearing is, k = W/R

where W is the supported weight and R is the length of the radius of curvature of the concave surface. This is the stiffness of a simple pendulum. The fact that the period of the Friction PendulumTM bearing is independent of the mass of the supported structure is an important property which has advantages in controlling the response of a structure. The desired period can be selected simply by choosing the radius of curvature of the concave surface. The period does not change for light or heavy structures, or if the weight of the structure changes or is different than assumed. The damping is controlled by the hysteretic dynamic friction which also automatically adjusts for uncertainties or changes in structure mass. This ability of the bearing to automatically adjust for uncertain or added structure mass improves safety. Larger than expected bearing displacements, that would otherwise occur with larger than expected structure masses, are avoided.

Tension Capacity

EPS offers a cylindrical version of our Friction Pendulum-TM bearing, that can carry tension loads. This bearing typically has two orthogonal cylindrical rails interconnected by a housing-slider assembly. The housing slider assembly contains two cylindrical sliders, and the housing unit which structurally interconnects the two orthogonal rails. When loaded in compression this cylindrical bearing has the same pendulum based seismic isolation properties, including period stiffness, and friction damping, as the spherical bearing. However the cylindrical tension bearing also maintains the pendulum based seismic isolation properties while carrying tension loads. The cylindrical tension bearing allows free multi-directional shear movements as with the non-tension spherical bearing. Bearing tension capacity provides overall structural connectivity and integrity. The cylindrical bearing is also available with a single rail, permitting sliding movements in one direction, while restraining against movement in the perpendi direction.

Performance and Quality Assurance Testing

The performance and properties of Friction PendulumTM isolators have been supported by extensive testing at internationally renowned earthquake engineering research centers, including: the National Center for Earthquake Engineering Research (NCEER), State University of New York at Buffalo (now known as MCEER); and the Earthquake

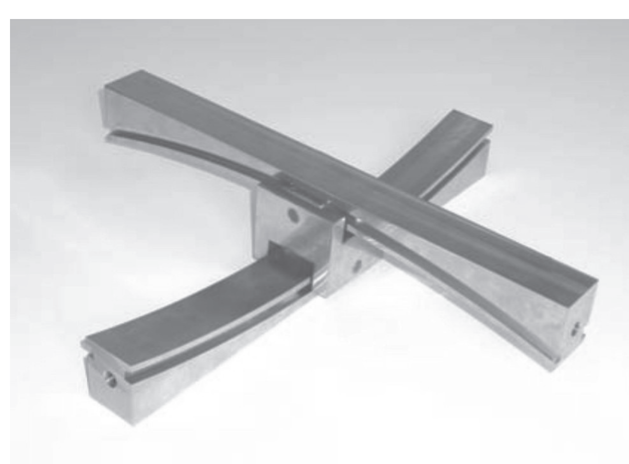

Tension Bearing

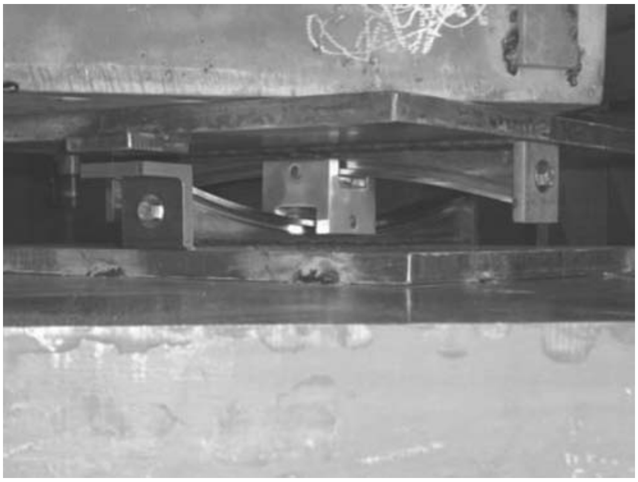

Tension Bearing in Test Machine

Engineering Research Center (EERC), University of California, Berkeley. The experimental hysteretic loops demonstrate an ideal bi-linear response of the Friction PendulumTM with no observable degradation under repeated cyclic loadings. The test results of full-size bearings for the U.S. Court of Appeals building show that Friction PendulumTM isolators retain their full strength and stability throughout their displacement range [9,17]. Friction damping reduces the seismic displacements. The dynamic friction is measured from tests of full-size isolators. The dynamic friction coefficient is calculated by dividing the area of the hysteretic loop by the total displacement travel. The break-away friction is measured during the first movement of the tests. The dynamic friction values from tests of full-size isolators were within 20% of the specified value. Break-away friction is typically equal to, or less than, the dynamic friction value. Under no circumstances did the break-away friction exceed the specified dynamic friction value by more than 20%. The behavior and response of Friction PendulumTM isolators to a wide range of earthquake loadings and superstructure types have been investigated both experimentally and analytically. Physical properties of the bearings are well established and exhibited a high degree of consistency throughout the entire series of test programs.

The performance and design of the Friction PendulumTM isolation system for the U.S. Court of Appeals was verified with shake table tests of unreinforced masonry structural models at the Earthquake Engineering Research Center, in August 1992. The isolated models were subjected to over

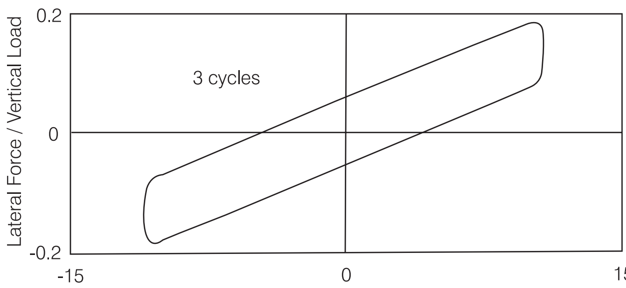

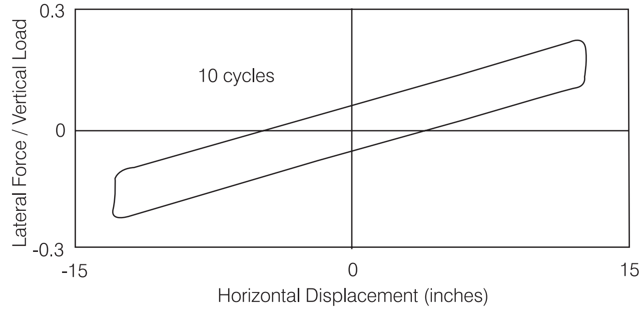

Test Results for 3 and 10 Cycles, respectively, at 1.2x Design Displacement

200 earthquake tests, including large, magnitude 8 earthquakes, without sustaining any damage to the masonry panels. The isolation bearings were then locked in place, and the non-isolated structural model was tested. After 3 small magnitude earthquakes, all of the masonry panels in the non-isolated structure were severely damaged, and testing was stopped.

Shake table tests carried out at the National Center for Earthquake Engineering Research in 1991 investigated the response of a 7 story steel framed structure having various lateral load resisting systems. Friction PendulumTM seismic isolators reduced the structure base shears, story shears, and story drifts in this test structure by factors of 4 to 6. These tests showed that the Friction PendulumTM isolators were effective in reducing the earthquake loads on multi-story structures having a large overturning aspect ratio and with different structural configurations.

The dynamic analysis models used to predict the behavior of the isolated structures have been verified with the results of shake table tests performed at EERC and NCEER. Comparisons of analysis models with test results show that the analysis results reliably and accurately predict the response of Friction PendulumTM isolated structures.

Torsion Properties

Their pendulum properties make Friction PendulumTM

EPS Test Machine

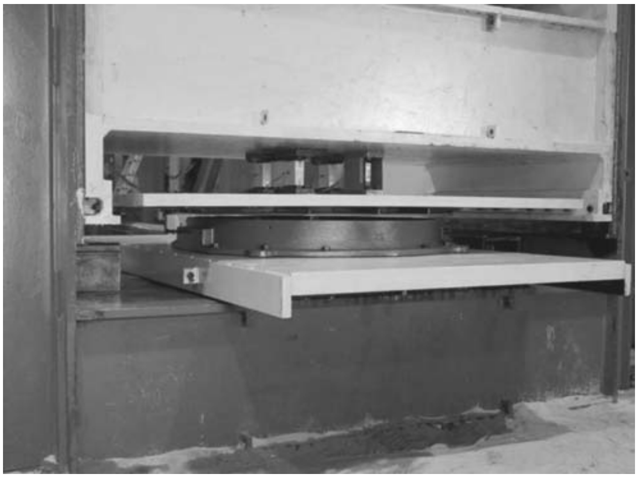

Bearing in Test Machine

bearings particularly effective at minimizing adverse torsion motions which result from accidental mass eccentricities. The bearing's dynamic stiffness is directly proportional to the supported weight, so that the center of lateral stiffness of the bearings always coincides with the center of mass. Since the friction force is also proportional to the supported weight, the center of the friction forces of the bearing group also coincides with the center of mass of the structure. Hence, the stiffness and friction forces automatically adjust for accidental mass eccentricities. Shake table tests have shown that these torsion properties significantly reduce torsion motions and stresses in the structure, improving structure safety, and reducing bearing displacements at the isolator level [7, 15, 16, 17]. Smaller isolator displacements reduce seismic gap requirements and expenses.

1992 URM Tests: Isolated structure remains undamaged after 58 earthquakes including magnitude 8 earthquake loadings.

Bearing Compression Strength

Friction PendulumTM bearings offer strength and stability that exceed those of any other seismic isolation bearing. An isolator from the U.S. Court of Appeals project in San Francisco, was compression load tested to nine times its design vertical load at the design lateral displacement and at the centered position. The bearing was then cyclically tested under compression and shear, and the results show the bearing retained its operational ability for lateral stiffness, damping, and vertical load capacity.

Individual bearings can support service level loads of 30 million pounds. Moreover, the bearings retain high strength factors of safety above the service load capacities. Vertical earthquake motions and seismic overturning moments make the bearing's vertical load factors of safety a critical life safety consideration. Bearings which resist seismic overturning moments experience the maximum vertical loads when they are at the maximum lateral displacement. While laterally displaced, the bearings must also sustain additional vertical loads due to vertical earthquake motions. Furthermore, the reduced vertical stiffness of the bearing, occurring at the design lateral displacement, increases the dynamic amplification of vertical motions, further increasing bearing loads. The vertical earthquake motions can increase bearing vertical loads by factors of 2 or more and should be accounted for in the design. During the Northridge Earthquake, dynamic amplifications ex-

1992 URM Tests: Non-Isolated structure fails after 3 earthquakes of magnitudes 5, 6 and 7, respectively.

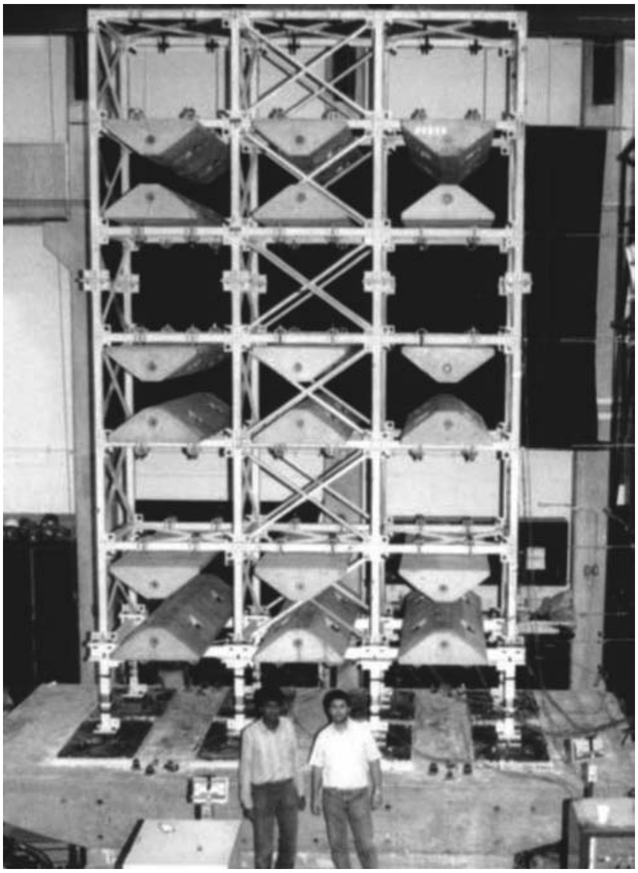

1991 Shake Table Tests of 7 Story Frame

ceeding 2 were observed for the vertical seismic motions within buildings supported with elastomeric bearings. Vertical bearing loads due to vertical earthquake motions are usually not explicitly accounted for in the UBC and ASHTO seismic isolation guidelines. To adequately resist vertical earthquake motions and other load uncertainties, EPS recommends the isolation bearings should provide strength factors of safety for compression loads of at least 2.0 at the maximum lateral displacement. UBC and ASHTO seismic isolation guidelines and typical seismic isolation designs with elastomeric bearings have required a vertical load factor of safety of only 1.0 at the maximum lateral displacement. Under combined vertical and lateral earthquake motions, a low strength factor of safety can result in overturning and collapse of the structure during the design seismic event. The most important life safety consideration in the design of seismic isolation bearings is vertical load stability in the laterally displaced position; at this position, isolation bearings perform their intended function and support their maximum loads.

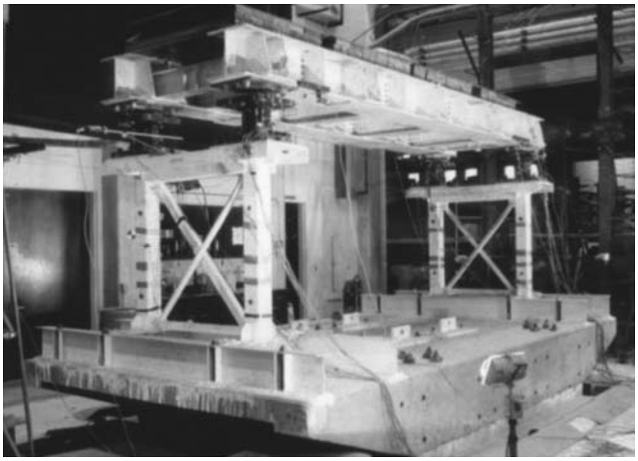

1992 Shake Table Tests of Bridge on Flexible Piers

Compression Stiffness

The compression stiffness of the Friction PendulumTM bearings is typically about 7 to 10 times greater than elastomeric isolation bearings. Most importantly, Friction PendulumTM bearings retain these vertical stiffness values at their design lateral displacement. Typical elastomeric isolation bearings have approximately one half the vertical stiffness at the design displacement as compared to the undeformed position. Thus, the vertical stiffness that resists the overturning moment loads is about 14 to 20 times greater for Friction PendulumTM bearings than that of elastomeric bearings. This higher vertical stiffness minimizes loss of the structure's shear wall stiffness due to rocking about the base, reduces uplift displacement demand on the bearings, and reduces the need for spreader trusses or walls across the base of the building to spread out the overturning moments. These factors can significantly reduce the isolator installation costs. The higher vertical stiffness of the Friction PendulumTM also results in a lower vertical period, which is less susceptible to dynamic amplification of the vertical motion. The vertical period of a typical Friction PendulumTM bearing is approximately 0.03 sec. From the UBC spectra, the dynamic amplification factor is 1.3. The vertical period of the typical elastomeric bearing, at the design lateral displacement, is approximately 0.1 sec. with a dynamic amplification factor of 2.0. The lower dynamic amplification factor for the Friction PendulumTM bearing reduces vertical bearing loads due to vertical earthquake motions, improving vertical load stability and safety as compared to the specified elastomeric design.

Unscragged and Scragged Properties

Scragging is the repeated lateral loading of an isolation bearing, to achieve a softening of the bearing stiffness. Elastomeric isolation bearings typically recover 70 to 90% of the unscragged properties within 3 months to 2 years after scragging. EPS recommends that structure shear force designs be based on unscragged bearing properties, which are measured from three or fewer cycles of lateral loading to the design lateral displacement applied to a previously untested bearing. Multiple cycles of loading at lesser displacements have a progressive scragging effect and should be avoided when measuring design stiffness and shear values. Basing the structure shear force design on stiffness properties measured after significant prior loading results in unconservative designs. Averaging four or more cycles of loading has a similar unconservative

Year	Location	Description	Principal Investigator	Ref. No.
1986	EERC	Compression-shear tests of model bearings.	Prof. Mahin	16
1986	EERC	Shake table tests of 2-story steel frame structure. Test Structures modeled full-size buildings with periods ranging from 0.3 to 3.0 sec. and torsional eccentricities of 0% to 45%	Prof. Mahin	16
1989	EERC	Compression-Shear testing of model low friction bearings at velocities up to 20 inches per second.	Prof. Mahin	15
1989	NCEER	Shake table tests of a 6-story steel moment frame (quarter scale model) using bearings below a rigid base.	Prof. Constantinou	7,8
1989	NCEER	Compression-shear tests of model bearings.	Prof. Constantinou	7
1990	EERC	Compression-Shear tests of full-size 2.0 sec. bearings used in the seismic retrofit of a 4-story apartment building.	Dr. Zayas	13
1990	NCEER	Shake table tests of a rigid slab bridge on bearings.	Prof. Constantinou	
1991	NCEER	Shake table tests on 7-story steel moment and braced frame buildings (quarter scale) with bearings below individual columns.	Prof. Constantinou	1,17
1992	EERC	Shake table tests of unreinforced brick/granite masonry panels using full-size 2.5 sec. period bearings.	Prof. Mahin	9,17
1992	NCEER	Shake table tests of a highway bridge on flexible piers with the bearings isolating the bridge deck from the piers.	Prof. Constantinou	6
1993	EERC	Compression-Shear testing of full-size 2.75 sec. period bearings. Vertical loading 44 to 1275 kips; sliding velocities from 0.1 to 20 inches per sec.; temperatures from –20°F to 90°F; simulated aging to 100 years.	Dr. Zayas	3,17
1994	NCEER	Shake table tests of computer equipment supported on bearings.	Prof. Constantinou	27
1995	NCEER	Tests of temperature, longevity and reliability using model bearings.	Prof. Constantinou	29
1997	ETEC	HITEC Compression-Shear tests and 10,000 cycle wear tests of full-size bearings for Caltrans and the Federal Highway Administration (FHWA).	Armand Onesto	30
1999	EERC	Caltrans shake table tests with bi-directional interaction for bridge applications.	Prof. Mahin	31
1999	NCREE Taiwan	Shake table tests of model bearings for use in power transmission towers.	Prof. Shinozuka	
2000-2001	UCSD	Caltrans High Speed Compression-Shear tests of large (13 feet diameter) bearings for retrofit of the Benicia-Martinez Bridge.	Prof. Seible	
2001	WA State Univ.	Shake table tests of a three story structural model with FP bearing and dampers (NSR Grant project).	Prof. Symans	
2001	UCSD	Caltrans, High Speed Compression-Shear tests of large Cylindrical Uni-directional FP bearing for retrofit of West Span of Oakland Bay Bridge.	Prof. Seible	32
2001	UCSD	Government of Turkey, Bolu Viaduct Project, High Speed Compression-Shear Prototype tests on large FP bearings.	Prof. Seible	33
2001	UCSD	Tennessee DOT, I-40 Project High Speed Compression-Shear tests of large FP bearings with vertical loads of up to 10,000 Kips	Prof. Seible	34
2002	MCEER	Shake table tests of cylindrical tension bearings	Prof. Constantinou	35

The following table lists chronologically the research test programs on the Friction PendulumTM seismic isolation bearings performed at University and Government sponsored laboratories.

effect. The first cycle of loading on each new virgin bearing tested for the U.S Court and the Revithoussa LNG Tanks, was recorded and reported, as were the subsequent loading cycles. The Friction PendulumTM bearings demonstrated relatively consistent stiffness and damping properties for either unscragged (virgin) or scragged (previously loaded) bearings. The first cycle of lateral loading on the virgin bearing resulted in friction coefficients approximately 1/2 % higher than those obtained from subsequent cycles. The first cycle virgin properties did not effect the tangent stiffness values. The bearings satisfied the design stiffness and damping requirements for the first and subsequent loading cycles. Since first cycle unscragged properties are stiffer than subsequent cycle properties, they result in higher seismic shear forces in the structure above. For the U.S. Court of Appeals and Revithoussa LNG Tanks, the first cycle properties were used for the structure shear force designs. Since the subsequent cycle properties are less stiff, the subsequent cycle properties were used to check maximum bearing displacement requirements. This approach results in a conservative design for both structure seismic shear forces and bearing displace-ments.

Temperature Effects

Low temperatures increase the stiffness of isolation bear-

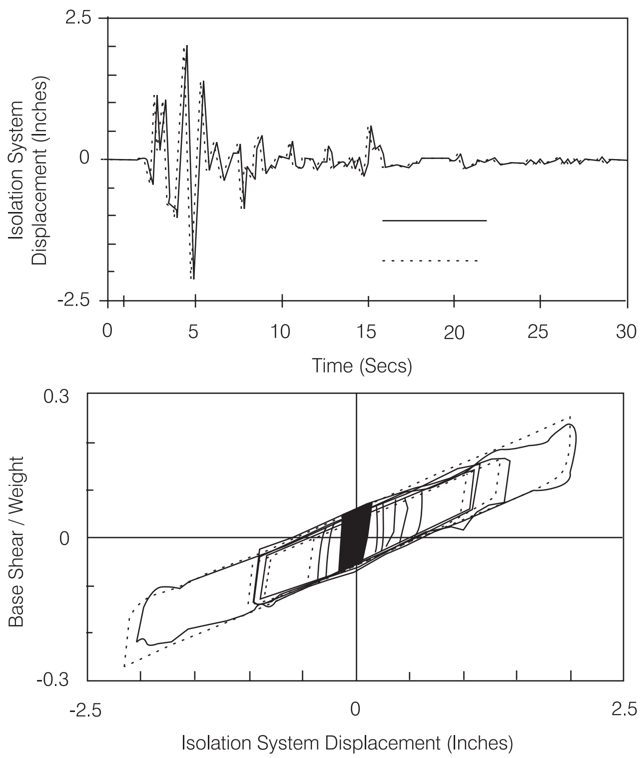

Comparison of Experimental Results and Analytical Prediction

ings, and high temperatures reduce the stiffness. This applies to both elastomeric and sliding bearings. EPS recommends that the structure shear force design be based on the cold temperature bearing properties, as applicable to the structure site. Since tests of material samples can produce significantly different results for temperature effects as compared to tests of full size bearings, EPS recommends that bearing temperature effects be based on tests of full size bearings. In order to quantify the effects of temperature on the properties of Friction PendulumTM isolators, full-size isolators were cooled or heated to the target temperatures at the bearing core, then subjected to combined compression and shear testing. A full-size bearing was cooled to -70 °F, then tested as the temperature gradually rose. Another bearing was heated to 90 °F, then tested as the temperature gradually lowered. The aerospace bearing liner is rated for operation from temperatures ranging from -320°F to +400 °F. The temperature tests showed that friction decreases as the temperature rises, and increases as the temperature decreases. There is no effect of temperature on the bearing dynamic stiffness or period. There is a small effect of temperature on the effective stiffness and period due to the friction coefficient change.

Material Longevity and Aging

The sliding interface components of the Friction PendulumTM bearing are constructed of materials with demonstrated longevity and resistance to environmental deterioration and aging [20, 21, 22, 23]. The bearing liner is a high strength, self-lubricating composite material that was developed for use in critical aerospace applications. It meets stringent specifications for use in military applications [21]. The concave sliding surface is a high grade stainless steel with exceptional corrosion and environmental resistance. The durability and long-term material reliability of Friction PendulumTM bearings result in an expected bearing life exceeding 100 years.

The principal properties that affect the performance of seismic isolation bearings are the stiffness, period, and damping. For Friction PendulumTM bearings, the stiffness and period are controlled by the radius of curvature of the concave surface. The radius of curvature does not change with time. Aging effects on the dynamic stiffness and period of the Friction PendulumTM bearings are, therefore, not significant.

The bearing liner is a high load/low friction composite, which provides non-degrading and low friction sliding, without the use of liquid lubricants. This composite material has been used in the U.S. aerospace industry for over 35 years for high load/high torque bearing applications. The rated static load capacity is 60,000 psi. The rated operating temperature range is -320°F to +400 °F. It provides much higher strength and wear durability than the PTFE materials used in typical bridge or structural bearings.

U.S. aerospace applications of this bearing material have very demanding performance and quality control requirements. They include: wing pivot bearings, landing gear bearings, helicopter blade bearings, aircraft engine bearings; and bearings in actuator systems for hydraulics systems; among others. The load requirements in the U.S. military aerospace applications are similar to, or exceed, those of the Friction PendulumTM bearings. Furthermore, the wear requirements exceed those of the Friction PendulumTM bearings.

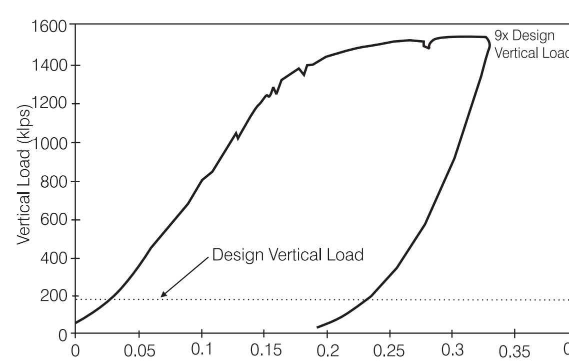

Compression Load Test at Lateral Displacement of 11 inches

U.S. Military Specifications set no age limit or shelf life limit for the use of this bearing material. The bearing material components have been identified as chemically stable and inert, with no noticeable effect of aging. A ten year old sample of the bearing material has been tested and found to show no noticeable deterioration due to age. It's resistance to industrial chemicals is rated as excellent.

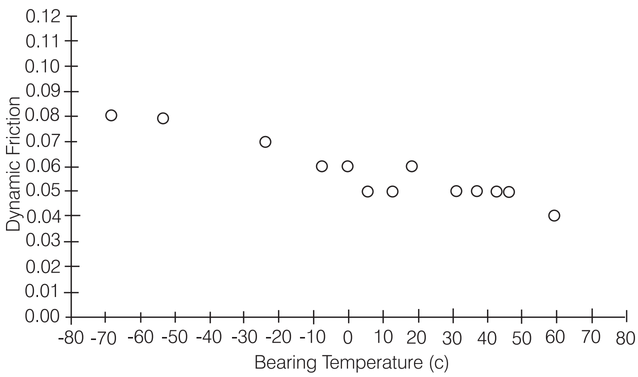

Effect of Temperature on Dynamic Friction

The other component of the sliding interface is the main stainless steel concave surface. ASTM A240 stainless steel, austenetic grade 300 series with a polished finish, is used for the concave surface.

The "Corrosion of Stainless Steels" section of the Metals Handbook Ninth Edition, Vol. 13 Corrosion, ASM International, reports results of observed corrosion of AISI 300 series stainless steels in a marine atmosphere [24]. Stainless steel samples were left exposed for 15 years, 250 meters from the sea. After 15 years, the Type 316 stainless steel exhibited extremely slight rust stains on 15% of the surface. The rust stains were easily cleaned to reveal a bright surface, and would have only a minor effect on the surface roughness and friction coefficient. For a sealed Friction PendulumTM bearing, installed in a building, similar rust stains would take more than 50 years to develop. Changes in the surface roughness of the concave surface have a modest effect on the dynamic friction value, primarily in the first cycle of loading.

To simulate long term aging effects, Friction PendulumTM bearings were tested with different surface roughnesses, including high mirror polish, low polish, and no polish. The tests were correlated to aging based on the ASM exposure tests, and stainless steel exposure tests by Taylor Devices [20] of stainless steel samples with outdoor and indoor exposure times ranging from 10 to 39 years. The no polish specimen included surface contamination from the steel mill, and was considered a conservative simulation of the worst case 100 year aging effect.

The effects of the simulated 100 year aging are shown in the figure on the following page. The figure shows the friction coefficients measured in the first cycle of loading. The 100 year simulated aged bearing demonstrated a 1% increase in the friction coefficient, as compared to the high mirror polish bearing. The friction increase was observed only for the first cycle of loading. Friction results for subsequent cycles were equivalent to the polished bearings.

The dynamic friction values of full-size bearings have remained within specification when subjected to repeated loadings during a single test, or over a series of earthquake tests, reaching the design life of the bearings. The wear life of Friction PendulumTM bearings exceeds thirty design basis earthquake loadings. The friction coefficients of bearings subjected to more than fifty cycles of loading in a single test, and more than fifty sequential earthquake loadings have remained stable and within the design specification.

The test results for the Friction PendulumTM composite bearing liner differ from those for soft PTFE materials used in typical structural and bridge bearings. The softer materials creep and impregnate themselves into the mate plates, causing break-away friction values that exceed the dynamic friction values [26]. In contrast, hundreds of tests on Friction PendulumTM bearings demonstrate the static break away friction coefficient is consistently less than, or equal to, the dynamic friction coefficient [1, 7, 15, 16, 18].

Moreover, Friction PendulumTM bearings were selected for the Revithoussa LNG Tanks over elastomeric bearing types, because they demonstrated the ability to satisfy the stringent performance requirements set for the effects of aging, temperature, and virgin (unscragged) properties. All bearings were required to satisfy the seismic performance requirements under the combined effects of 35 years aging, low temperatures of 10°F, and virgin unscragged properties, as well as the combined effects of new bearing properties, high temperatures of 86°F, and scragged run-in properties. Satisfaction of these performance requirements were required to be demonstrated by performing full-size bearing tests under the specified range of conditions. Elastomeric bearings were tested, but were not able to satisfy the performance requirements. Friction PendulumTM bearings satisfied all performance requirements.

Fire Resistance

The Friction PendulumTM bearing offers the innate fire resistance of heavy steel joints. Bearings for bridges typically weigh from 2000 to 10,000 lbs, making a concentrated mass which heats slowly, and maintains stability at temperatures exceeding 1500°F. The aerospace bearing liner can withstand temperatures of 600 °F without damage, and maintains operational ability up to 400°F. All materials are non-combustible, except for the ethyleyne propylene seal which can withstand temperatures up to 350°F. The seal is replaceable after a fire if needed.

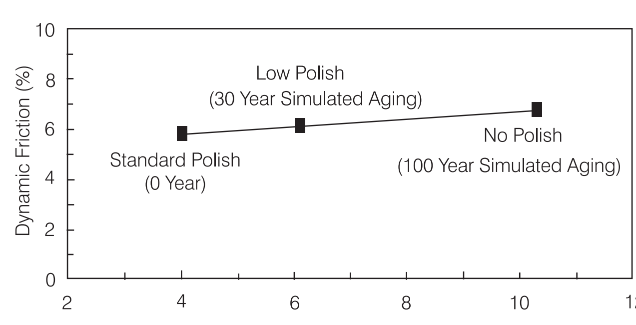

Effect of Aging

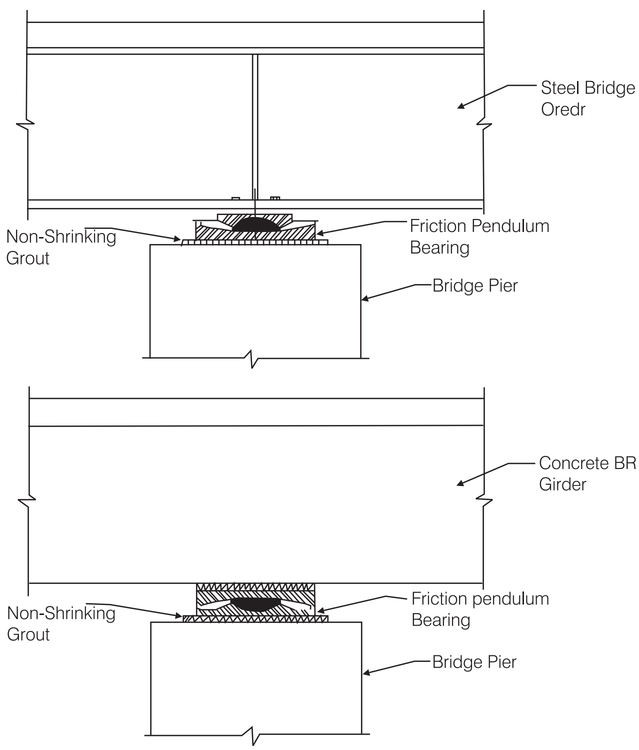

Typical Installation Details

The bearings can be fire protected using standard fire protection methods for structural steel members. The exterior may be field sprayed with standard fire proof aggregate. Prior to spraying, the bearing's seismic movement joints should be fitted with expansion joint material to allow bearing movements.

The bearing can also be supplied with pre-encased fire board, which can meet the fire rating requirements of an individual project. The fire board is fitted to allow bearing seismic movements, and is removable and replaceable.

Installation Details and Requirements

The Friction PendulumTM bearings offer many installation benefits compared to elastomeric bearings:

- The bearing does not require upper or lower base plates. This saves base plate material costs, handling costs, and installation time.
- The FP bearing is vertically stiff, minimizing the vertical deflections of columns that occur during bearing installation in retrofit applications. This avoids damage to architectural finishes in the upper floors, and reducing bearing installation time and cost.
- In retrofit applications, the FP bearing does not require flat jacks. This results in savings in flat jack costs and installation time.
- The low profile bearing can be installed in constrained locations, saving foundation and structure disruption costs and time.
- The FP bearing connection can be welded, offering flexibility and cost savings in connection details.
- The tension and side plates of the FP bearing provide the necessary temporary lateral force resistance needed during construction, avoiding the cost, time and space constraints of installing temporary bracing.
- The bearings can be installed with the concave surface facing either up or down. P-Delta moments are avoided for the structural members below the isolator, when the concave surface is facing down. This reduces the seismic forces transmitted to the foundation. P-Delta moments are avoided for the structural members above the isolator when the concave surface is facing up. This reduces the seismic forces transmitted to the upper structure.

The installation benefits of the Friction PendulumTM bearings have saved millions of dollars in project construction costs and time.

The compact Friction PendulumTM bearing can accommodate constrained and difficult installation conditions. This often results in substantial savings in the costs of construction installation details.

The relatively small height of the Friction PendulumTM isolator makes it preferable for installation in constrained crawl spaces, or at elevator and stair locations. The isolators are vertically rigid, retaining their full height after installation and loading. This avoids long-term creep concerns.

The isolators can be installed either with the concave surface facing up or down. The articulated joint allows relative rotations between the structure above and below the isolators, and reduces the isolator moment loads on the structure. P-Delta moments are avoided for the structural members below the isolator, when the concave surface is facing down. P-Delta moments are avoided for the structural members above the isolator when the concave surface is facing up. The cylindrical retainer ring of the Friction PendulumTM provides a redundant support system capable of supporting the full design vertical and lateral loads.

Friction PendulumTM isolators need less clear space around them to allow for isolator distortions. Only the sliding plane of movement needs to be accommodated. These installation details offer important advantages at locations such as exterior or interior walls, elevators, stairs, or entry ways. Seismic gap details are simplified because the slight rise of the isolators as they laterally deflect lifts overlapping plates in seismic gap joints away from expansion gap materials.

Author Affiliation

Victor Zayas

Ph.D., P.E., President, Earthquake Protection Systems, Inc, California, USA.

References

1. Al-Hussaini, T.M., Zayas, V.A., Constantinou, M.C., "Seismic Isolation of Multi-Story Frame Structures with Friction Pendulum Isolators", Technical Report 94-007, National Center for Earthquake Engineering Research, State University of New York at Buffalo, 1994.
2. Al-Hussaini, T.M., Zayas, V.A., Constantinou, M.C., "Seismic Upgrade of Multi-Story Buildings Using the Friction Pendulum Isolation System", Proc., Tall Buildings in Developing Countries, International Conference on Tall Buildings, Dhaka, Bangladesh, June, 1993.
3. Amin, N., Mokha, A. and Fatehi, H., "Rehabilitation of the U.S. Court of Appeals Building Using Sliding Isolation System", Proc., ATC-17-1 Seminar on Seismic Isolation, Passive Energy Dissipation and Active Control, Applied Technology Council, San Francisco, March 1993.
4. Zayas, V.A., Constantinou, M.C., Tsopelas, P. and Kartoum A. "Testing of Friction Pendulum Seismic Isolation Bearings for Bridges." Proceedings of the Fourth World Congress on Joint Sealing and Bearing Systems for Concrete Structures, Sacramento, California, September 1996.
5. Constantinou, M.C., Mokha, A.S., and Reinhorn, A.M., "Teflon Bearings in Base Isolation II: Modeling" Journal of Structural Engineering, American Society of Civil Engineers, Structural Division, Vol. 116, No. 2, 1990.
6. Constantinou, M.C., Tsopelas, P., Kim, Y-S. and Okamoto, S., "NCEER-Taisei Corporation Research Program on Sliding Isolation Systems for Bridges: Experimental and Analytical Study of Friction Pendulum System", Report No. 93-0020, National Center for Earthquake Engineering, State University of New York at Buffalo, Nov. 1993.
7. Mokha, A.S., Constantinou, M.C., and Reinhorn, A.M. "Experimental Study and Analytical Prediction of Earthquake Response of a Sliding Isolation System with a Spherical Surface" Report No. NCEER 90-0020, National Center for Earthquake Engineering Research, State University of New York at Buffalo, October 1990.
8. Mokha, A.S., Constantinou, M.C., Reinhorn, A.M. and Zayas, V.A., "Experimental Study of Friction Pendulum Isolation System." Journal of Structural Engineering, American Society of Civil Engineers, Structural Division, Vol. 117, No. 4, April, 1991.
9. Zayas, V.A., and Low, S. "Seismic Isolation Retrofit of a Historic Building", Proceedings of National Earthquake Conference, Central United States Earthquake Consortium, Memphis, Tennessee, May 1993.
10. Zayas, V.A., and Low, S.S., "Earthquake Resistant Design Using Friction Pendulum Connections." Seismic Engineering: Research and Practice, The American Society of Civil Engineers, Structures Congress, San Francisco, May 1989.
11. Zayas, V.A., and Low, S.S., "A Simple Pendulum Technique For Achieving Seismic Isolation." Earthquake Spectra, Professional Journal of the Earthquake Engineering Research Institute, May 1990.
12. Zayas, V.A., and Low, S.S., "Seismic Isolation Retrofit of an Apartment Building." The American Society of Civil Engineers, Structures Congress, Indianapolis, April 1991.
13. Zayas, V. and Low, S., "Application of Seismic Isolation to a Four Story Wood Building", 1991 SEAOC Proceedings, SEAOC Convention, 1991
14. Zayas, V.A., and Low, S.S., "Seismic Isolation Retrofit of an Historic Building", 1993 National Earthquake Conference, Memphis, Tennessee, May 1993.
15. Zayas, V., Low, S., Bozzo, L. and Mahin S., "Feasibility and Performance Studies on Improving the Earthquake Resistance of New and Existing Buildings Using the Friction Pendulum System", UCB/EERC-89/09, Earthquake Engineering Research Center, University of California, Berkeley, 1989.
16. Zayas, V.A., Low, S.S., and Mahin S.A. "The FPS Earthquake Resisting System, Experimental Report." Report No. UCB/EERC 87/01, Earthquake Engineering Research Center, University of California, Berkeley, June 1987.
17. Zayas, V., Piepenbrock, T. and Al-Hussaini, T., "Summary of Testing of the Friction Pendulum Seismic Isolation System: 1986-1993", Proc., ATC-17-1 Seminar on Seismic Isolation, Passive Energy Dissipation and Active Control, Applied Technology Council, San Francisco, March 1993.
18. Zayas, V.A., Low, S.S., and Mahin S.A., "Shake Table Testing of a Friction Pendulum Seismic Isolation System." Seismic Engineering: Research and Practice, The American Society of Civil Engineering, Structural Congress, San Francisco, May 1989.
19. Zayas, V.A., Low, S.S., Mahin, S.A., "Seismic Isolation Using the Friction Pendulum System." The 10th International Conference On Structural Mechanics in Reactor Technology, Anaheim, California, August 1989.
20. Soong, T.T. and Constantinou, M.C. (1994). Passive and Active Structural Vibration Control in Civil Engineering, Springer-Verlag, Wien-New York.
21. Gardos, M.N. (1982). Self -lubricating Composites for Extreme Environmental Applications, "Tribology International, October, 273-283.
22. Bowden, F.P. and Tabor, D. (1964). The Friction and Lubrication of Solids. Part II, Oxford University Press.
23. Derjaguin, B.V. and Toporov, Y.P. (1982). "Influence of Adhesion on the Sliding and Rolling Friction," in Microscopic Aspects of Adhesion and Lubrication, edited by J.M. Georges, Tribology Series 7, Elsevier Scientific Publishing Co.

24. ASM International (1987). Metals Handbook, Vol. 13 on Corrosion, Metals Park, Ohio.

25. International Nickel Company (1963). "Corrosion Resistance of Austenitic Chromium-Nickel Stainless Steels in Atmospheric Environments.

26. Mokha, A., Constantinou, M.C. and Reinhorn, A.M. (1991). "Further Results on the Frictional Properties Bearings," J. Struct. Engng., ASCE, 117(2), 622-626.

27. Lambrou V. and Constantinou, M.C. "Study of Seismic Isolation Systems for Computer Floors." Technical Report NCEER-94-0020, National Center for Earthquake Engineering Research, State University of New York at Buffalo, July 1994.

28. Zayas, V.A., Constantinou, M.C., Tsopelas, P. and Kartoum A. "Testing of Friction Pendulum Seismic Isolation Bearings for Bridges." Proceedings of the Fourth World Congress on Joint Sealing and Bearing Systems for Concrete Structures, Sacramento, California, September 1996.

29. Constantinou, M.C. "Research on Longevity and Reliability of Sliding Seismic Isolation Systems.", NCEER Highway Project Technical Report, National Center for Earthquake Engineering Research, State University of New York at Buffalo, 1996.

30. CERF Report: HITEC 98-07 #40370 "Evaluation Findings for Earthquake Protection Systems, Inc. Friction Pendulum Bearings" September 1998.

31. Madden, G.J., Symans, M.D., and Wongpraset, N. (2002). "Experimental Verification of Seismic Response of Building Frame with Adaptive Sliding Base Isolation System," J. of Structural Engineering, ASCE, Vol. 128, No. 8.

32. Seible, F., UCSD Test Report on Uni-directional Cylindrical FP bearings for retrofit of West Span of San Francisco-Oakland Bay Bridge, 2001.

33. Seible, F., UCSD Prototype Test Report on FP bearing for Bolu Viaduct Project for government of Turkey, 2001.

34. Seible, F., UCSD Test Report of FP bearings for retrofit of I-40 project, Tennessee DOT, 2002.

35. Constantinou, M.C., MCEER Shake table tests of cylindrical tension bearings.

Advanced Models for Condition Survey and Inspection Planning of RC Structures in Marine Environment

K. Balaji Rao[1] and M. B. Anoop[2]

Abtract

Chloride induced corrosion of reinforcement in reinforced- and prestressed- concrete structures is a problem of national importance since enormous costs involved in the inspection and maintenance of these structures. There is an urgent need to develop scientific and more rational methodologies, leading to optimal inspection scheduling and efficient maintenance regimes, and, implement the same in management systems. This paper presents some of the efforts made at CSIR-SERC. For the first time, it is shown how the Polya Urn model can be used for rational decision making regarding the corrosion state estimation of RC girders in a bridge stock. It is also shown how this model will help in condition assessment (with respect to prestress loss) of prestressed concrete girders in a bridge stock, using data from monitoring of strains on limited number of girders.

Keywords

Chloride induced corrosion, Condition assessment, Inspection scheduling, Polya Urn

Introduction

The performance of constructed facilities created using reinforced concrete (RC), has clearly indicated that these structures have finite life and the life of similar structures exposed to nominally similar environment vary. Due to variations in loads incidenting on the structure, resistance of structural components and the usage of the structure during its service life, the life of a reinforced concrete structure should at least be considered as a random variable. Hence, the best an engineer can view, at the design stage, is expected life and the design life of the structure. While the expected life of the structure is the mean life, design life can be construed as the desired value (i.e. characteristic value) of the life.

The performance requirements for a service life design has been stated in the CEB-FIP Model Code 1990 as: "Concrete shall be designed, constructed and operated in such a way that, under the expected environmental influences, they maintain their safety, serviceability and acceptable appearance during an explicit or implicit period of time without requiring unforeseen high costs for maintenance and repair" (fib, 1999). CEB has decided in 1996 to accept a performance-based approach with explicit attention for the design life, limit states and reliability.

In 1996, the three year DuraCrete project, partly funded by European Union, has started with partners from owners of structures, design engineers, contractors and binder manufactures. The main objectives and targets of the DuraCrete projects are

- Define a probabilistic framework for developing a design basis for durability
- Establish/propose deterioration models taking into account the uncertainty of environmental and material parameters
- Quantify effects of different compliance tests on predictions of lifetime performance
- Suggest a safety format for design for durability which complies with safety requirements

In the DuraCrete project, existing degradation models are used to formulate a new performance based durability design code. Using this design code, it will be possible to model the future time dependent performance (durability) of a concrete structure. The knowledge from this project has been used in the service life design of Western Scheldt tunnel (Netherlands). This is the first concrete structure that has been designed completely on the basis of service life, performance and reliability. Other practical applications of service life design include the Great Belt Link (Denmark) and the Oresund Link Bridge (between Denmark and Sweden). Corrosion of reinforcement is identified as the main deterioration process for concrete structures in the DuraCrete project and the new design methodology aims primarily to handle corrosion and the mechanisms leading to corrosion.

It is clear from the above that a realistic service life prediction of RC structures with respect to corrosion of reinforcement in concrete should take into account the possible damage scenarios and also the random variations in severity of exposure conditions (around the specified environmental conditions). When time to corrosion initiation is considered as the useful life of the structure, the damage state corresponding to initiation would result in costly remedial measures. However, if corrosion propagation is accepted, depending upon the loss of area of reinforcement, the damage state of the structure varies. For example, the consequences of loss of area due to corrosion as given by CEB are presented in Table 1. Thus, it is now possible to integrate the existing limit state design clauses with service life design criteria. Also, depending upon the accepted level of damage, the allocation of resources (also can be viewed as loss) varies.

Visual Indications	**Area Ratio**		
	$\approx$ 0.95	$\approx$ 0.90	$\approx$ 0.75
Colour changes	Rust stains	Rust stains	Rust stains
Cracking	Several longitudinal Some on stirrups	Extensive	Extensive
Spalling	Some	Extensive	In some cases, steel is no more in contact with concrete

Table 1. Damage levels of reinforced concrete structural elements subjected to corrosion of reinforcement given by CEB (Andrade et al., 1990)

While the DuraCrete project aims at establishing a rational durability based design procedure, there is also a need for evolving rational procedures for condition assessment of existing structures using NDT/NDE data and assessment of remaining life of the RC structures. It is to be noted that the field investigations carried out on the constructed facilities have clearly brought out the need for understanding the various degradation mechanisms when the structures are exposed to different environments. Both field investigations (mostly NDT) and laboratory tests have been conducted to understand the degradation processes/mechanisms and attempts are also being made to develop suitable models which can be used to quantify the same.

Another important aspect to be considered while assessing safety of existing prestressed concrete bridges is the time-dependent prestress losses due to creep-, shrinkage- of concrete and relaxation in prestressing steel during the service life. The inadequate performances of a number of prestressed concrete bridges (Bazant et al., 2008, 2012) have brought to the focus the need for reliable estimation of prestress losses, which is required to ensure the safety and serviceability of these structures during their service life. While number of models have been proposed by various codal committees/researchers for creep- and shrinkage- of concrete, most of these models do not takes into consideration the random variations in environmental and system parameters affecting the creep- and shrinkage- of concrete. Due to these variations, the remaining prestress in prestressed concrete structural components at any time also show variations. Development of methodologies for condition assessment of prestressed concrete bridges, taking into account these variations implicitly or explicitly, is an area of active research world wide. Development of such methodologies will help in more rational scheduling of inspection/maintenance activities and in realizing sustainable structures. Studies in this direction are being carried out at CSIR-SERC.

From the above discussion it is clear that maintenance must be considered at the design stage for the new structures, while for existing structures, more rational models for condition assessment and inspection planning need to be developed. This aspect becomes more important in the context of development of sustainable infrastructure (Trinius and Sjöström, 2007). This paper aims at presenting some of the probabilistic/stochastic prediction models developed to estimate the condition of the RC structure and thus helping in rational planning of inspections. The application of Polya urn model for corrosion state assessment of RC bridge girders is proposed for the first time in this paper. The usefulness of this model for condition assessment (with respect to prestress loss) of prestressed concrete girders in a bridge stock is also illustrated.

Figure 1 presents schematic of the research carried out at CSIR-SERC in this area.

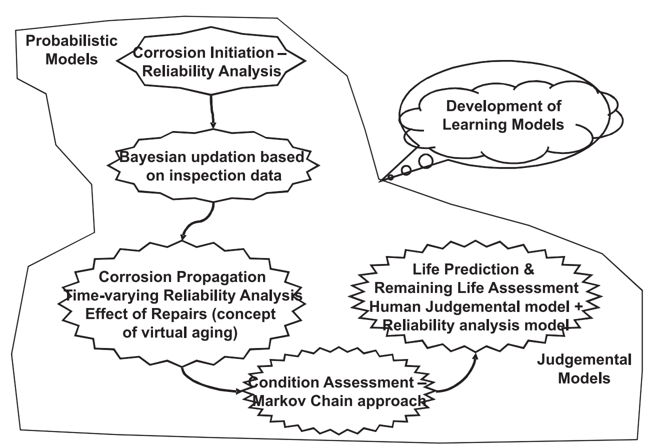

Fig. 1 Studies at CSIR-SERC on condition assessment

Markov Chain Modelling for Condition Assessment of Rc Bridge Girders

A methodology based on Markov Chain (MC) for condition assessment of RC bridge girders based on limited data obtained during principal inspection has been proposed (Balaji Rao and Appa Rao, 1999). The MC model is applied to determine the corrosion and/or cracking state of the bridge girders based on limited set of observations. In order to elucidate the formulations related to MC model, the example of corrosion state of reinforcement in a bridge girder is considered here. However, by properly defining state space, the model can be generalised for assessment of condition of girders with reference to other possible damages also.

The corrosion state of a reinforcing bar (at a given depth from top) in a specified bridge girder, exposed to a given nominal environmental conditions, is a random variable. The corrosion state of the reinforcing bar (at the same specified depth from top) also varies along the length of the bridge (i.e. from one girder to the other). Thus, the corrosion state of the reinforcing bar in a bridge has to be modelled as a random process. In this study, a MC model is developed with the state space as the corrosion state of the reinforcing bar in the girder and the index space as the girder number along the length of the bridge. In developing the model, the following assumptions are made:

The bridge girders are exposed to homogeneous environment (i.e. the severity of the environment is same for all girders, at specified location in the bridge), and the corrosion state of bar in any given girder depends only on the corrosion state of the bar in girder adjacent to it.

For the problem considered, the state space contains only two values namely, 0 (non-corroded state) and 1 (corroded state). The index space is characterised by the number of girders along the length of the bridge {1,2,…,n}. Thus, the state of (reinforcement of) adjacent girder depends on the state of present girder only and not on states of other previous girders. The stochastic evolution of the states of system is completely described by Transition Probability Matrix (TPM), which is a 2x2 matrix for the present problem.

Application

A typical field visual observation of a sequence of 10 adjacent girders of a bridge is given in Table 2. A MC is constructed for modelling the occurrence of girders with corroded reinforcement. The transition probability matrix (TPM) governing the stochastic evolution of the process is constructed based on the sampling observations given Table 2. Using the MC model, the following cases are studied:

Case 1. The percentage of girders in the whole bridge that would have corroded reinforcement: Using the TPM constructed, the percentage of girders with corroded reinforcement = 22 percent. In arriving at this probability, the one step dependence of the state of the reinforcement has been considered. However, if this dependence is not considered, the probability of finding a girder with a corroded reinforcement = 2/10 = 0.20. Hence, above type of formulation is more rational.

Case 2. The average number of girders to be inspected before a distressed girder (i.e., a girder with corroded reinforcement and/or having a visible crack) is observed, if the first girder inspected is free of corrosion and visible cracks: The average number of girders to be inspected before a distressed girder is observed is determined as 2.5. The result indicates that, on the average about 3 adjacent girders have to be inspected from the present girder, which is not distressed, to come across a distressed girder. This type of inference will be useful in conducting detailed inspection of bridge girders based on limited observations obtained during principal inspection.

Case 3. The average number of girders to be inspected before a girder with a corroded reinforcement and with no visible cracking is encountered, if the first girder inspected is free of corrosion and visible crack: It is found that starting from the first girder, on the average 7 more adjacent girders have to be inspected to encounter a girder with corroded reinforcement and not containing any visible cracks. This type of analysis helps in planning of inspections during principal inspection. Also, the results give an idea about relative damage/distress distribution among girders of bridge.

Girder number	Corrosion state	Presence of visible cracks
1	No	No
2	No	No
3	Yes	No
4	Yes	Yes
5	No	Yes
6	No	No
7	No	No
8	No	No
9	No	Yes
10	No	Yes

Table 2 Typical field visual observations of a RC bridge girder (Balaji Rao and Appa Rao, 1999)

Polya URN Model for Corrosion Assessment of RC Bridge Girders

One of the important factors that need to be considered while evolving models for carrying out condition assessment of overall structural component/structure, using limited data from of field investigations, is the large deviations that can be expected in the predictions made. The model to be used should identify explicitly the value of quantity of information of a given type. Keeping these in view, the Polya urn model is selected.

Polya urn model is a type of birth process. In a Polya urn model, there are two types of balls: black and white ones. In a basic step, one ball is selected randomly from the urn, which is then returned to the urn together with an additional ball of the same color. As noted by Antal et al. (2010), since the balls can represent anything from atoms to biological organisms to humans, urn models are widely used in the physical, life, and social sciences.

A methodology for corrosion state assessment of RC bridge girders based on limited data obtained from principal inspection is presented here.

Let n be the number of girders examined during the principal inspection. Let B represent the number of girders with no corrosion and W represent the number of girders with corrosion. Then n = B + W, and the initial configuration on the Polya urn is (B, W). Suppose N is the number of girders in the entire bridge stock (N ≥ n). It is assumed that the girders in the bridge stock considered are exposed to nominally similar environment (can be characterised using the Environmental Aggressiveness Factor (Anoop et al. (2002)). The objective is to make predictions regarding the corrosion state of the girders in the bridge stock using the limited inspection data. This can be achieved using the Polya urn model. For instance, suppose one is interested in determining the probability that exactly 50% of the girders in the entire bridge stock have corroded reinforcement. This can be determined using the first passage probability relation proposed by Antal et al. (2010) as:

$$G_n(B,W) \cong A(B,W)\left(\frac{N}{2}\right)^{-2}; \quad \frac{N}{2} >> B,W \tag{1}$$

Where

$$A(B,W) = \frac{(B-W)(B+W-1)!}{(B-1)!(W-1)!}2^{-B-W} \tag{2}$$

Figures 2 and 3 show the typical sample paths corresponding to two different quantities of initial field information; the first configuration is (9,1) and the second is (90,10). It may be noted that in both the cases, the relative frequency of the number of corroded girders are equal (i.e., 10%), while the number of girders inspected are different (10 and 100, respectively). Suppose there are 1000 bridge girders in the bridge stock (i.e., N = 1000). The probabilities that exactly 50% of the girders in the entire bridge stock are corroded for the both cases are obtained, using Eq. 1, as 2.81x10-7 and 3.93x10-20, respectively. Such inferences will be useful in making decisions regarding the detailed inspection and allocation of funds for inspection/repair.

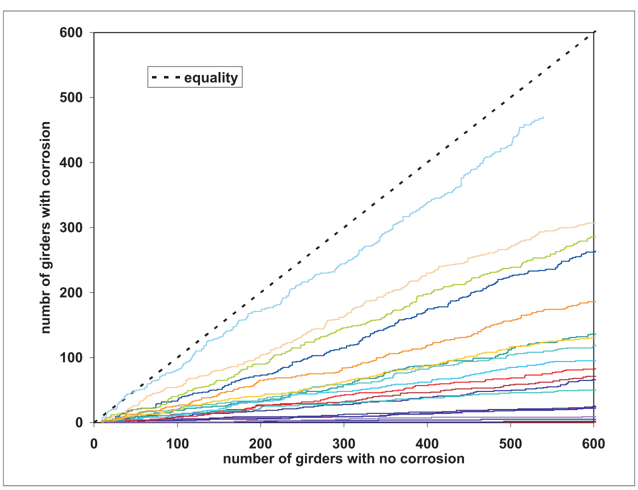

Fig. 2 Typical sample paths for the configuration (9,1)

While the MC model addresses the problem of condition assessment when inspection data from adjacent girders are available, the Polya urn model addresses the same when the inspection data is from randomly selected girders exposed to nominally similar environment.

Example: Polya Urn Model for Condition Assessment of Prestressed Concrete Bridge Girders

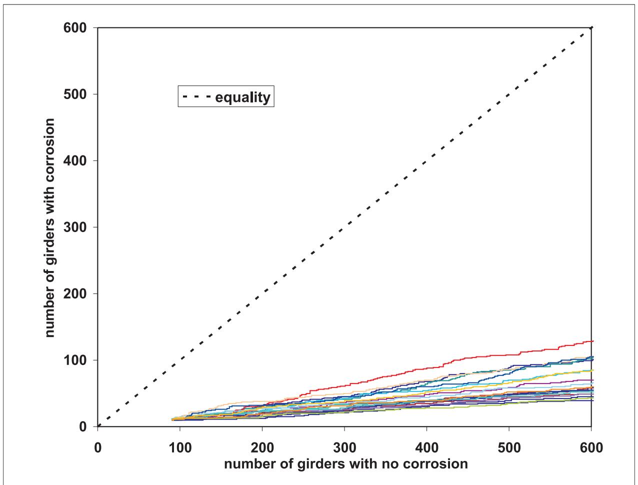

Fig. 3 Typical sample paths for the configuration (90,10)

A Polya urn model is proposed for condition assessment (with respect to prestress loss) of prestressed concrete bridge girders in a bridge stock, using data from monitoring of strains in limited number of girders. Let ‘n’ be the number of girders examined/monitored for strains, ‘B’ be the number of girders with prestress losses less than the admissible prestress loss at time ‘t’, and, ‘W’ be the number of girders with prestress losses more than the admissible prestress loss at time ‘t’. Then n = B+W, and the initial configuration of the Polya urn is (B, W).

It is assumed that the girders in the bridge stock considered are exposed to nominally similar environment, and the number of girders in the entire bridge stock, ‘N’ is much greater than the number of girders examined (n). The objective is to make predictions regarding the condition of the girders in the bridge stock using the limited data. This can be achieved using the Polya urn model.

In this study, three initial configurations have been considered: namely (4,1), (11,4) and (14,6), to illustrate the effect of amount of information available on the condition assessment. Figure 4 shows the typical sample paths for three different initial configurations, each corresponding to different numbers of bridge girders examined/monitored for strains. Assume that there are 1000 nominally similar prestressed concrete girders in the bridge stock (N = 1000), and ‘n’ number of them are continuously monitored for strains. The expected prestress losses at any time ‘t’ is determined using ACI procedure along with B3 model for creep and shrinkage and ACI model for relaxation. The expected prestress losses estimated at the design stage are considered as the allowable losses, since these losses are considered in deciding the initial prestress. The probability that exactly 50% of the girders in the entire bridge stock would have prestress losses more than the expected prestress losses at any time ‘t’ is determined using the first passage probability relation (Eq. 1). These probabilities for the three initial configurations considered are shown in Fig. 5. Estimation of these probabilities will be useful for inspection scheduling by comparing with the value of acceptable

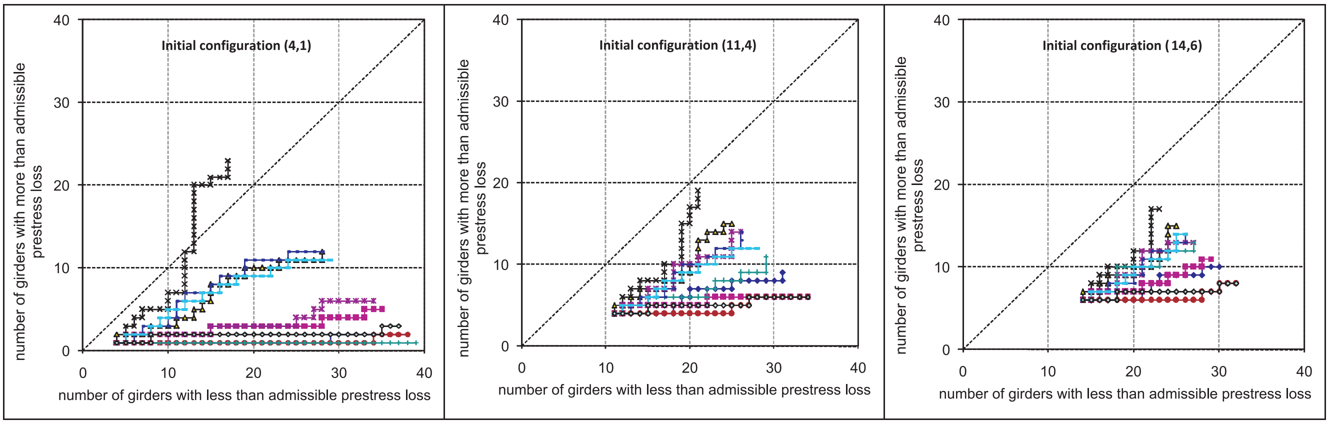

Fig. 4 Typical sample paths for three different initial configurations for the prestressed concrete bridge stock

probability (which needs to be decided by the codal committees/decision making authorities). The proposed model takes into consideration the value of information available, and hence helps in informed inspection scheduling.

Corrosion Initiation In Reinforced Concrete Bridge Girders Using Bayesian Technique

Development of reliability-based service life models require that the models can incorporate the information generated during in-service inspection; that is, the models/model parameters can be updated based on in-service inspection data. Use of Bayesian methods for incorporation of information obtained during in-service inspection in condition assessment and thus in realistic service life estimation of existing structures is well established (viz., Mori and Ellingwood 1994a, b). However, in most of the above investigations, conjugate distributions are used in decision making. While the use conjugate distribution helps in making the problem more mathematically tractable, it may not be possible to include the greater degree of engineering judgment in decision making regarding expected service life.

A methodology for the assessment of time of corrosion initiation in reinforced concrete bridge girders using Bayesian techniques is proposed (Balaji Rao et al., 2003). The methodology will be useful for realistic service life assessment

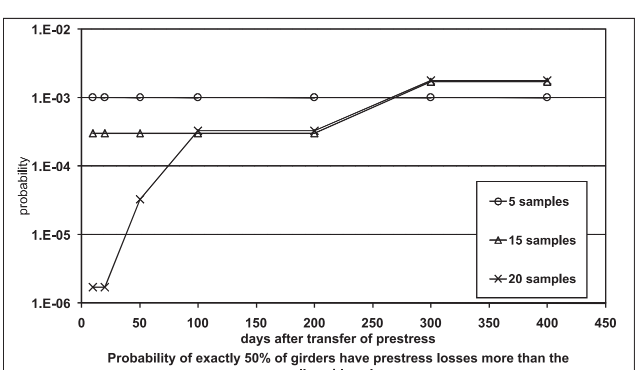

Fig. 5 Probability of exactly 50% of the girders in the bridge stock having prestress losses more than expected prestresses losses (estimated at the design stage using B3 model)

based on data from field inspection. Attempt has been made to show how engineering judgment can be used in formulating the likelihood function used in Bayesian decision making. The form of likelihood function is generally not known. Determination of the form requires engineering and statistical judgment or background. The form of likelihood function should be so chosen that it will in-crease the likelihood of observations made based on data obtained from field investigations. Likelihood functions were formulated for two different cases, which will arise in practice: i) in more number of cases the chloride concentration obtained from field investigation is less than the mean chloride concentration estimated earlier by the designer, and, ii) in more number of cases the chloride concentration obtained from field investigation is more than the mean chloride concentration estimated earlier by the designer. Effectiveness of the proposed methodology was demonstrated by applying it to the chloride concentration data obtained from field investigations on Gimsøystraumen Bridge, Norway (Fluge, 2001). From the measured chloride profiles at the end of 11 years, surface chloride concentration and diffusion coefficient values for 236 locations were determined and were reported in Fluge (2001). It is noted that out of the 236 observations, in 163 cases, the chloride concentration at the level of reinforcement determined based on field investigations exceeds the mean predicted by the designer, i.e., in more number of cases, the chloride concentration from field investigations is more than the mean chloride concentration estimated by the designer (case ii). From the three values of probability of corrosion initiation obtained, namely, 0.805 (based on the prediction at the design stage), 0.912 (based on the point estimate –computed using relative frequency approach- from information obtained from field investigations), 0.960 (based on updated chloride concentration using the proposed methodology), it is noted that the value obtained using the proposed methodology corroborates with the engineering decision taken to repair the bridge girder at the end of 11 years (Fluge, 2001). This also suggests that the forms of the prior distribution and the likelihood function used in this investigation are appropriate. Thus, the prediction made using the Bayes techniques is more realistic, and the use of proposed methodology helps in making better decisions (Fig. 6).

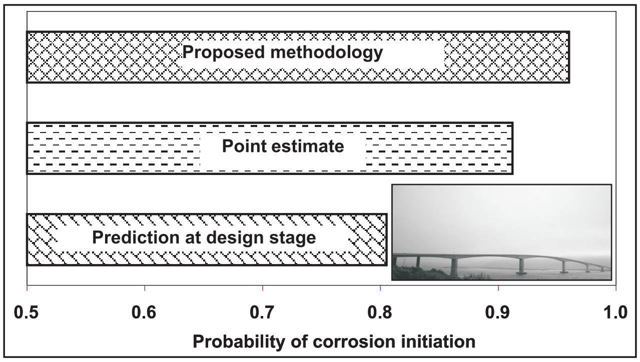

Fig. 6 Probability of corrosion initiation at the end of 11 years for the Gimsøystraumen bridge girder

Maintenance Scheduling for Corrosion-Affected Reinforced Concrete Structural Elements

The design of structure should take into account the possible degradation that may occur during its service life, thus facilitating the scheduling of maintenance activities (which can be optimised) and avoiding costly repairs/replacements. A methodology for maintenance scheduling, based on estimation of the reliability of corrosion affected reinforced concrete structural members taking into consideration the time and degree of repairs, is proposed (Balaji Rao et al., 2002). The methodology uses the concepts of virtual aging, failure rate and time-variant reliability analysis. Due to the repair, a part of the degraded resistance of the member is restored. The amount of restoration of resistance depends upon the degree of repair, z, defined as the ratio of restored resistance to the degraded resistance. The concept of virtual resistance ratio is used to take into account the effect of repair on the resistance of the member (see Fig. 7). The virtual resistance ratio at any time is considered as a random variable to take into account the stochasticity in the material properties, cross sectional dimensions and level of degradation. Since the virtual resistance ratio is bounded between zero and one, a truncated distribution is used for representing the variations in this quantity. The reliabilities of a 6m span simply supported beam subjected to chloride-induced corrosion of reinforcement was determined using the proposed methodology. The beam has been designed according to IS 456-2000 for moderate exposure conditions. However, in practice the beam was found to be exposed to severe exposure conditions. The reliabilities of the beam against different damage levels (see Balaji Rao et al. (2002) for definitions of damage levels) at different time intervals are computed. The reliabilities of the beam against damage state 3 (corresponding to 25% loss in area) are shown in Fig. 8. The methodology is general and can be used to estimate the reliability against any specified damage level. Knowing the required reliability levels against specified damage, it is possible to select the optimal time and degree of repair.

Modeling The Resistance Degradation of Reinforced Concrete Structures Due to Corrosion - A Fuzzy Methodology

CSIR-SERC, Madras, proposed a methodology for assessing the service life of reinforced concrete flexural members subjected to the chloride induced corrosion of reinforcement (Anoop et al., 2003). In practice, linguistic terms are used for characterising the exposure condition and quality of construction, and hence uncertainties arise. In the proposed methodology, these uncertainties are taken into account by considering the time to corrosion initiation, corrosion current and factor for including the effect of localized chloride-induced corrosion as fuzzy variables.

The efficacy of the proposed methodology is demonstrated through a practical case study by comparing the predicted times for different levels of damage due to corrosion of reinforcement (Table 1) to those reported for a severely distressed beam of the Rocky Point Viaduct. The time taken for the different levels of reduction in area ratio and the possible damages at these ages for the case study con-

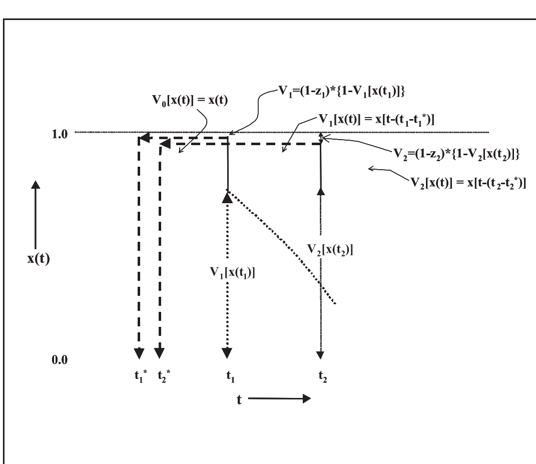

Fig. 7 Renewal process with perfect/imperfect repair

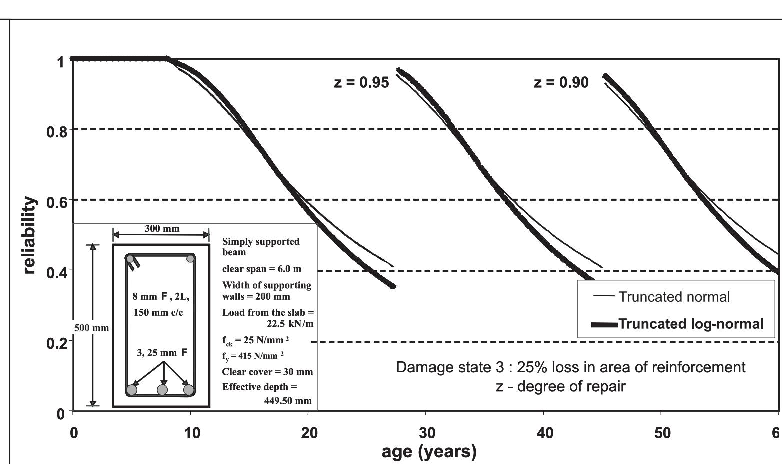

Fig. 8 Reliabilities for the beam against damage state 3

Area Ratio	Possible/expected damage (based on CEB proposal) [Andrade et al (1990)]	Observed time for the damage/ distress (years)*	Predicted time using the proposed methodology	
			Range (years)	Minimum time (years)
0.95	Rust stains; Several longitudinal cracking, some cracking on stirrups; Spalling - some	≈ 13	10.3 – 25.0	10.3
0.90	Rust stains; Extensive cracking and spalling	≈ 14	11.7 – 28.1	11.7

Note: * - obtained from inspection and maintenance records (Covino et al., 1999, Cramer et al., 2000)

Table 3. Time for different levels of damage for the beam considered in case study

sidered is given in Table 3. It is noted from Table 3 that the predicted times are in agreement with the observed time (obtained from inspection and maintenance records) for different damage levels. This shows the efficacy of the proposed methodology. The assessment of service life will be useful for decision making while designing the member.

Summary

Some of the probabilistic/stochastic prediction models developed at CSIR-SERC for condition estimation/assessment of the RC structures located in marine environment are presented in this paper. Application of these models will help in more rational planning of inspections/inspection scheduling for new- as well as existing- structures and hence improving sustainability. It is also shown for the first time how the Polya Urn model can be used for condition assessment, with respect to prestress loss, and inspection scheduling of prestressed concrete girders in a bridge stock. The proposed models can be used in expert systems for more rational management of structures.

Acknowledgements

This paper is published with the kind permission of the Director, CSIR-Structural Engineering Research Centre, Chennai. The first author is grateful to his Ph.D. thesis guide, Prof. Prakash Desayi, and, to Dr T.V.S.R. Appa Rao and Dr N. Lakshmanan, former directors of CSIR-SERC, Chennai, for giving the encouragement.

Author Affiliation

K. Balaji Rao[1] and M. B. Anoop[2]

Scientist, Risk and Reliability of Structures Group, CSIR – SERC, CSIR Campus, Taramani, Chennai, India.

References

- Andrade, C., Alonso, M.C. and Gonzalez, J.A. (1990), ‘An initial effort to use the corrosion rate measurements for estimating rebar durability’, Corrosion rates of steel in concrete, ASTM STP 1065, American Society for Testing and Materials, Philadelphia, 29-37.
- Anoop, M.B., Balaji Rao, K. and Appa Rao, T.V.S.R. (2003), ‘A methodology for durability-based service life design of reinforced concrete flexural members’, Mag. Conc. Res., 55 (3), 289-303.
- Anoop, M.B., Balaji Rao, K. and Appa Rao, T.V.S.R. (2002), ‘Application of fuzzy sets for estimating service life of reinforced concrete structural members in corrosive environments’, Engg. Strcut., 24 (9), 1229-1242.
- Antal, T., Ben-Naim, E. and Krapivsky, P.V. (2010), ‘First-passage properties of the Polya urn process’, Journal of Statistical Mechanics: Theory and Experiment, doi:10.1088/1742-5468/2010/07/P07009.
- Balaji Rao, K. and Appa Rao, T.V.S.R. (1999), ‘A methodology for condition assessment of rc bridge girders with limited inspection data’, The Bridge & Structural Engineer, Ing-IABSE, Vol. 29, No. 4, pp.13-26.
- Balaji Rao, K., Anoop, M.B. and Appa Rao, T.V.S.R. (2002), ‘Reliability analysis of stochastic degrading and maintained systems’, Proceedings of 6th International Conference on Probabilistic Safety Assessment and Management (PSAM6), San Juan, Puerto Rico, USA, June 23-28, 2002.
- Balaji Rao, K., Satish, B., Anoop, M.B., Gopalakrishnan, S. and Appa Rao, T.V.S.R. (2003), “Application of Bayesian technique for corrosion state assessment of reinforced concrete bridge girders”, in ‘Safety and Reliability’, Ed. T. Bedford, P.H.A.J.M. van Gelder, Proceedings of ESREL 2003, 15-18 June, 2003, Maastricht, The Netherlands, A. A. Balkema Publishers, pp. 73-80.
- Bazant, Z.P., Li, G-.H. and Yu, Q. (2008), ‘Explanation of excessive Long-Time Deflections of collapsed Record span Box Girder Bridge in Palau’. Preliminary report, 8th International conference on creep and shrinkage of concrete (CONCREEP-8), Ise-Shima, Japan.
- Bazant, Z.P., Li, G-.H. and Yu, Q. (2012), ‘Excessive Long-Time Deflections of Prestressed Box Girders. I: Record-Span Bridge in Palau and Other Paradigms’. J. Struct. Eng., ASCE, 138(6), 676–686.
- Covino, B.S., Cramer, S.D., Holcomb, G.R., Bullard, S.J. and Laylor, H.M. (1999), ‘Postmortem of a failed bridge’, Concrete International, 21(2), 39 – 45.
- Cramer, S.D., Covino, B.S., Holcomb, G.R., Bullard, S.J., Russel, J.H., Dahlin, C.M., Summers, C.A., Laylor, H.M. and Soltesz, S.M. (2000), Evaluation of Rocky Point Viaduct concrete beam, Report No. FHWA-OR-RD-00-18, Oregon Department of Transportation, Oregon.
- fib (1999), Structural Concrete: Textbook on behaviour, design and performance Updated knowledge of the CEB/FIP Model Code 1990 - Volume 3, International Federation for Structural Concrete, December 1999.
- Fluge, F. (2001), ‘Marine chlorides: A probabilistic ap-

proach to derive provisions for EN 206-1', In Service life design of concrete structures – from theory to standardization: 63-83. 3rd Duranet Workshop, Tromsø, Norway.

- Mori, Y. and Ellingwood, R. (1994a), 'Maintaining reliability of concrete structures. I: Role of inspection/repair', Journal of Structural Engineering (ASCE), 120(3), 824-845.
- Mori, Y. and Ellingwood, R. (1994b), 'Maintaining reliability of concrete structures. II: Optimum inspection/repair', Journal of Structural Engineering (ASCE), 120(3), 846-862.
- Trinius, W. and Sjöström, C. (2007). Sustainability in building construction – international standards in progress. Journal of ASTM International. Vol. 4, No. 7.

Innovative Empire State Building Program Saves Millions

The innovative energy efficiency program at the Empire State Building has exceeded guaranteed energy savings for the second year in a row, saving $2.3 million and providing a new model for building retrofits that is now being rolled out across the US.

In 2009, the Empire State Building, President Bill Clinton and Mayor Michael Bloomberg launched a comprehensive retrofit at the landmark property to reduce costs, increase real estate value and protect the environment. In 2011, the Empire State Building beat its year-one energy-efficiency guarantee by a remarkable 5 percent, saving $2.4 million. In year two, the iconic property surpassed its energy-efficiency guarantee by nearly 4 percent. As with the first year's results, all information and monitoring and verification reports can be viewed at www.Esbsustainability.com.

Rising Sun Taipei City Project Phases 1 and 2 Underway

The US$1.4 billion Rising Sun Taipei City development in Chongqing, China is being developed by the Rising Sun International Real Estate Venture Investment LLC. The project will include high-rise residential units, a four-storey shopping mall, a hotel, movie theatre, service apartments with retail facilities, mixed-use office and commercial units and related amenities.

The development will have over 1.09 million square meters of built-up area and will be built in nine phases."Phases I and II are already underway, while work is on the verge of starting for the remaining seven phases," said Robert Houser, Hill International's project director for the Rising Sun Taipei City development. "The aim is to complete the project by December 2016."

World's Tallest Building Breaks Ground in China

Broad Sustainable Building Co., LTD (BSB) that specializes in factory-made skyscrapers and a wholly owned subsidiary of Chinese major BROAD Group, intending to build the world's tallest skyscraper in a record time held a groundbreaking ceremony on July 20, in Chang sha, China. Broad Sustainable Building is planning to build the 838-meter (2,749-foot) Sky City using its prefabricated modular construction method. The founder of parent company Broad Group Chairman Zhang Yue announced the tower will be completed by April 2014 and will cost around ¥5.2 billion (US$846 million) to complete. Its total built-up area will contain just over 1 square kilometer (10 million square feet) of space.

The tower, which will be taller than Dubai's Burj Khalifa by 10 meters (33 feet), will contain a hotel for 1,000 guests and housing for up to 31,400 people, ranging from penthouses to high-density units for low-income tenants. It will also contain a hospital, schools, shops, restaurants and offices, creating an entire city within the building. According to a press release from Broad Group, 90 percent of the building will be pre-fabricated in the company's factories. The units will be produced by 20,000 workers in four months. Subsequently it will take three months for 30,000 workers to finish fabricating the units and other actual constructions on site.

USD 1.5 bn Sheraton Huzhou to Open Its Doors

The unusual 321-room Sheraton Huzhou Hot Spring Resort, located on the Taihu Lake between Nanjing and Shanghai, is set to open its doors. The oval-shaped, 27-story building was designed by MAD Architects and is being touted as one of Sheraton's most elaborate hotels. The $1.5 billion resort measures over 100 meters (328 feet) high and 116 meters wide (380 feet).

Google Street View Goes to Paris

A few weeks after Google took its Street View imagery to the top of the world's tallest building, the Burj Khalifa in Dubai; the Internet giant has turned its attention to the French capital, giving the same treatment to the city's majestic Eiffel Tower.

Google has not only uploaded a stack of panoramic imagery gathered from the Tower's three viewing platforms. The company has also mounted online exhibitions featuring images, plans, engravings and photographs detailing the story of the Eiffel Tower's development as well as its social impact in the 19th century.

"In order to capture the imagery, the Street View team followed in the footsteps of seven million annual visitors and ascended multiple floors of the Tower," Mark Yoshitake of the Google Cultural Institute wrote in a blog post introducing the new material. "Using the Street View Trolley (designed especially for monuments and museums) they filmed 360-degree views of the monument's architecture and its views over Paris."

Yoshitake said it's been "awe-inspiring to get to see the spectacular vision, and the detailed architectural capabilities exemplified by the plans more than 100 years ago. It required tremendous knowledge of special planning and physics to ensure that 18,000 separately made pieces would come together as one."

Google has said its application users can expect to see many more of the world's tallest structures popping up on Street View.

TELUS Launches Sky Tower by BIG

TELUS, one of Canada's largest telecommunications companies, is set to begin construction on a 58-story tower in Calgary's downtown core. The TELUS Sky tower, designed by Bjarke Ingels Group (BIG), will incorporate office space, retail stores and 341 residential rental suites.

The 750,000-square foot (70,000-square meter) building is expected to be completed by the fall of 2017 with an estimated price tag of US$400 million, according to The Calgary Herald.

"Our new development is a powerful contribution to Calgary's economic strength, culture and social vitality," Darren Entwistle, TELUS President and CEO said in the project press release. "TELUS Sky will enrich the city's vibrant arts culture by offering inspiring public spaces that will exhibit works of art by local artists, thus creating a truly amazing destination for our team members, the community and indeed all Albertans."

TELUS will be the anchor tenant of the building, occupying nearly a fifth of the building's square footage.

DMCC Proposes Next Tallest Commercial Tower

The Dubai Multi Commodities Centre (DMCC) announced on Tuesday it is planning to build what could ultimately be the tallest commercial tower in the world, in the Jumeirah Lakes Towers development. The company announced that the tower will be taller than the 508-meter (1,666-foot) Taipei 101, the world's current tallest completed office building.

"Building the world's tallest tower is in the Dubai DNA," Ahmed bin Sulayem, Executive Chairman of DMCC, told The National. "We will use the best technology, the best materials and the best designers in the world to bring this project to life."

The DMCC Business Park would comprise 107,000 square meters (1 million square feet) of commercial and retail space.

China's Government to Impose a Great Migration

The Chinese government is pushing a plan to move 250 million Chinese people from rural communities into newly constructed towns and cities over the next 12 years. These drastic steps create a Chinese urban population greater than most of the world's urban populations combined.

These steps include bulldozing ancient villages, temples and entire neighborhoods, as well as paving over farmland and forcing farmers to move in order to make way for mega-cities. By 2030, China will boast 13 mega-cities, those with population of 10 million or more, according to Bloomberg. China currently has six mega-cities.

Those who live in rural communities in China are largely self-sufficient, growing their own food and providing their own energy. Supporters of the move argue that rapid urbanization and a shift from production to consumption will create new opportunities for construction companies, transportation, utilities and appliance makers.

"If half of China's population starts consuming, growth is inevitable," Li Xiangyang, Vice Director of the Institutes of World Economics and Politics, told the New York Times. "Right now they are living in rural areas where they do not consume."

Prince Alwaleed Bin Talal plans to pursue another supertall

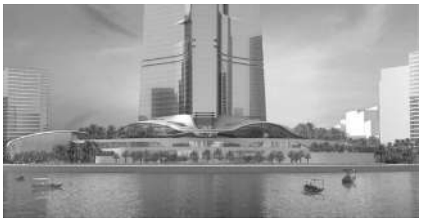

Saudi billionaire Prince Alwaleed Bin Talal announced that plans to build the Kingdom Tower in Jeddah, Saudi Arabia are on schedule, taking the opportunity to express interest in building a higher tower in another city, perhaps as tall as one mile (1.6 kilometers). The board of directors of Jeddah Economic Company (JEC) met in Riyadh to discuss the Kingdom's progress.

The board reported that piling work has begun for the SAR4.6 billion (US$1.2 billion) Kingdom Tower. The prince called on Emaar and Chairman Mohammed Alabbar to enter a joint venture with his JEC to pursue another Supertall somewhere in the world. "Right now we are discussing and evaluating the possibility of building a one-mile tower," Mr. Alwaleed told reporters."I am now inviting the major cities of the world like Shanghai, Moscow, New York, London and regional cities in the Middle East to come and give their offers."

New York Was Once Under an Enormous Mountain Range

The BBC profiles Professor Iain Stewart, a geologist at Plymouth University in the UK, as he studies the incredible bedrock that has made possible Manhattan as we know it. The minerals in this rock, known as schist, provide clues to America's ancient geologic history and places in context the bedrock that anchors many of the world's earliest and best-known skyscrapers.

In the four part series Rise of the Continents, Professor Stewart follows and explains the formation of continents and how that changed human history. The minerals indicate that the city's bedrock was formed at the bottom of a mountain range."The former mountains of New York probably achieved heights similar to what we see in the Himalayas today, it's incredible to imagine mountains 15 times higher than highest skyscraper on the skyline today," Professor Stewart explains. "It's amazing to think that the modern city of New York has essentially been controlled by geology below and all that started with the construction of Pangaea."

One World Trade Center Tops Out

A silver spire weighing 758 tonnes has been attached to the roof of One World Trade Centre (OWTC) in New York completing the construction of the tallest building. The building is 1,776 foot (541.3 m) in height. The 124 m spire will serve as a world-class broadcast antenna. An LED-powered light emanating from it will be seen from miles away. The addition of the spire, and its raising of the building's height to 541 metres, makes One World Trade Center the tallest structure in the US and third-tallest in the world. If the building does not have the spire, One World Trade Centre would actually be shorter than the Willis Tower in Chicago, which stands at 442.26 metres and has the title of tallest building in the US, not including its own antennas. The tower is due to open for business in 2014.

Strawscraper an Urban Power Plant in Stockholm

Belatchew Arkitekter presents Strawscraper, the first project to come out of the newly established Belatchew Labs. Strawscraper is an extension of Söder Torn on Södermalm in Stockholm with a new energy producing shell covered in straws that can recover wind energy. What was supposed to become a building of 40 flights became 26. Söder Torn on Södermalm in central Stockholm was finalized 1997, but the architect Henning Larsen had already left the contract after having lost influence over the design of the tower.

Belatchew Arkitekter wants to give Söder Torn its original proportions and at the same time explore new techniques that could create the urban wind farm of the future. By using piezoelectric technology a large number of thin straws can produce electricity merely through small movements generated by the wind. The result is a new kind of wind power plant that opens up possibilities of how buildings can produce energy. With the help of this technique surfaces on both old and new buildings can be transformed into energy producing entities.

Furthermore, an additional aspect is revealed when the constant movement of the straws creates an undulating landscape on the facades. What is usually considered to be the most static of all things, the building, suddenly comes alive and the construction gives the impression of a body that is breathing. The straws swaying in the wind gives the building a constantly changing facade further reinforced at night time with lighting in changing colors. The straws of the facade consist of a composite material with piezoelectric properties that can turn motion into electrical energy. Piezoelectricity is created when certain crystals' deformation is transformed into electricity. The technique has advantages when compared to traditional wind turbines since it is quite and does not disturb wildlife. It functions at low wind velocity since only a light breeze is sufficient for the straws to start swaying and generate energy.

The existing premise on top of the building is replaced with a public floor with room for a restaurant. The new extension creates, a part from the energy producing shell, room for the citizens with the possibility to reach a lookout platform at the very top of the tower with an unmatched view of Stockholm.

Panamanian inventor unveils new parachutes for occupants in high-rise buildings

A Panamanian inventor has demonstrated a new parachute, which can open after just 100 feet (31 meters) to be used as an escape option for people in high-rise buildings during a catastrophe. The SOS Parachute by Morris Shahbazi can open more quickly and at lower heights than most similar devices. The parachute has been through 13 tests, and all have functioned properly. Mr. Shahbazi said he was inspired by the 2001 attacks on the World Trade Center, in which hundreds of people were left stranded atop the burning buildings.

Others have cautioned that problems remain with the idea, including the role of wind at high altitudes, as well as the possibility of dozens of people attempting to use and open their chutes at once.

Australian research team develop silent turbine system

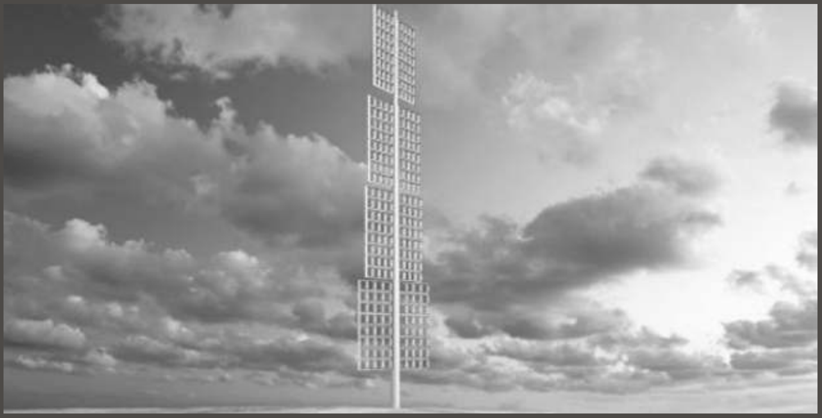

A team from Australia's University of Wollongong (UOW) under the direction of Professor Farzad Safaei has developed Power WINDows, a new type of wind-to-energy converter. The modular turbines were developed to keep noise vibration and operating costs to a minimum.

The system is composed of an array of small panels arranged in a grid. Each panel is a miniature turbine itself, which moves up and down with the direction of the wind, unlike traditional turbines, which run perpendicular to it. The wind panels generate less noise and less turbulence, and place less stress on the supporting structure. The turbines also turn more slowly than is typical, and are more visible, which will help birds to avoid the spinning blades.

AS+GG Wins Imperial Tower Competition

Adrian Smith + Gordon Gill Architecture have won Mumbai's Imperial Tower competition with a 400-meter aerodynamic design. The Imperial Tower, which could become the tallest in the city, was designed to "confuse the wind" by minimizing the negative effects of wind in the low-rise city.

In addition to its curved profile, the tower's sky gardens will also contribute to mitigating currents, the residential tower will include apartments ranging in sizes from 72 to 1,115 square meters (775 to 12,000 square feet).

A Suspended Night Club Tower Proposed for Hong Kong

Architecture firm Urbanplunger has created a proposal for a nightclub and hotel tower in Hong Kong that would be completely suspended above the ground. The structure, which would lean on neighboring buildings' infrastructure, acts as an "architectural parasite.

The building is connected to the ground level green space by only a series of glass elevators which lead to the nightclub on the lowest levels. Above that is a public lobby, which provides access to a spa, swimming pool, restaurants and a business cent. The upper-level hotel would feature balconied rooms as well as a presidential suite at the top.

2013

2nd International Conference on Civil Engineering and Architecture (ICCEA 2013)

August 10-11, 2013, Barcelona, Spain

IACSIT and International Journal of Engineering and Technology (IJET)

ICCEA 2013 E-mail: iccea@iacsit.net

ICCEA 2013 www.iccea.org

The 30th International Symposium on automation and Robotics in Construction and Mining

August 11 - 15, 2013 | Montreal, QC, Canada

General Chair: Ferri Hassani

fhassani-isarc@isarc2013.org

www.isarc2013.org

International Conference on Sustainable Construction Materials & Technologies (SCMT3)

August 18 - 21, 2013 | Kyoto, Japan

www.scmt.org.uk

Structural Mechanics in Reactor Technology (SMiRT-22)

August 18 - 23, 2013 | San Francisco, CA

Information : info@smirt22.org

www.smirt22.org

6th CECAR (Civil Engineering Conference in Asia Region)

August 20, 2013 to August 22, 2013

Hotel Borobudur, Jakarta, INDONESIA

E-mail: iswandi@si.itb.ac.id; info@cecar6.com

Phone: 62-22-2510715

Fax: 62-22-2512403

Our World in Concrete & Structures

August 22 - 23, 2013 | Singapore

Tel: +65 67332922

Fax: +65 62353530

Email: ci-p (at) cipremier.com

www.cipremier.com/page.php?663

The Best Show in Public Works

August 25 - 28, 2013 | Chicago, IL

www.apwa.net/congress

CPRI PortsTM '13

August 25 - 28, 2013 | Seattle, Washington

CC2013 The Fourteenth International Conference on Civil, Structural and Environmental Engineering Computing

September 3-6, 2013, T-Hotel, Cagliari, Sardinia, Italy

Civil-Comp Ltd, Scotland (UK).

Tel: +44 (0)1786 870166 fax: +44 (0)1786 870167

Email: registration@civil-comp.com

Transformables 2013

September 18 - 20, 2013, Seville, Spain

Emilio Pérez Piñero died fifty years ago. In his honor the First International Conference Transformables2013 is being organized with the aim of advancing in the research, design and building ideas on Transformability, Modularity and Lightness. Architects, Engineers, Artists, Academics

www.iass-structures.org

The 2013 IASS Annual Symposium with the theme "Beyond the Limit of Man"

23 - 27 September, Wroclaw, Poland

www.iass-structures.org

26th IABSE Symposium: Long Span Bridge and Roof Structures - Development, Design and Implementation

24 - 27 September, Kolkata, India (Annual Meetings precede Symposium)

www.iabse.org

The 23rd Annual Louisiana

Civil Engineering Conference & Show

September 25-26, 2013 | Kenner, Los Angels

www.louisianacivilengineeringconference.org/

2nd International Symposium on UHPFRC

2 - 4 October, AFGC Marseille, France

www.afgc.asso.fr

The sixth conference on Textile Composites and Inflatable Structures (structural Membranes 2013)

October 09 - 11, 2013, Technical University of Munich, Germany

www.iass-structures.org

ASCE - 143rd Annual Civil Engineering Conference
Civil Engineers - The Foundation of the Nation

October 9-12, 2013 | Charlotte, North Caroline

ACI Fall 2013 Convention

October 20, 2013 to October 24, 2013

Hyatt Regency & Phoenix Convention Center, Phoeniz, AZ USA

E-mail: Renee.Lewis@concrete.org

Phone: (248) 848-3794

Fax: (248) 848-3701

www.aciconvention.org

Carbon Management Technology Conference

October 21-23, 2013

Hilton Alexandria Old town Alexandria, Va

www.fscarbonmanagement.org

Innovative World of Concrete ICI-IWC 2013
International Conference on Innovations in Concrete for Meeting Infrastructure Challenges

October 23 - 26, 2013

Hitex / NAC, Hyderabad, Andhra Pradesh, India

2nd T&DI Green Streets, Highways and Development Conference

November 3 - 6, 2013 | Austin, Texas

www.content.asce.org/conferences/greenstreets-highways2013

3rd International Conference on Urban Public Transportation Systems

November 17 - 20, 2013

National Conservatory of Arts and Crafts, Paris, France

Tel: (703) 295-6014,

E-mail: kking@asce.org
www.content.asce.org/conferences/tdi/utsconference/index.html

International Colloquium on Architecture Structure Interaction for Sustainable Built Environment

November 18-20, 2013 | India Habitat Centre, Lodhi Road, New Delhi, India

SEWC 2013 Symposium International Symposium on Innovative Architecture-Structure interaction towards Sustainable Development with Green environment

25-27 November, New Delhi.
Email: scmehrotra@mehroconsultants.com

1st R N Raikar Memorial International Conference

December 20, 2013 to December 21, 2013, Mumbai, India

Dr. Surendra K. Manjrekar
E-mail: info@sunandachemicals.com, skmanjrekar@gmail.com
Phone: 91-22-24034130
Fax: 91-22-24034133
Www.ic-aci-rnraikarmemorialinternationalconference.com

4th International fib Congress fib group India

10-14 February, Mumbai, India and Exhibition

ASEC 2014 - Structural Engineering in Australasia World Standard

Sky City Auckland, New Zealand from Wednesday 9 July to Friday 11 July 2014

The conference will provide a unique environment to facilitate discussion and debate between New Zealand, Australian and international colleagues from around the world. This conference will bring together professionals from a broad range of disciplines, including architecture, structural engineering, seismology, geology, geophysics, geotechnical engineering, business, public policy, social sciences, regional planning, emergency response planning and regulation. The extreme weather and earthquake events experienced in both countries in recent years provide fertile ground for learning.

5th International Conference on Concrete Repair

September 1, 2014 to September 3, 2014
Wellington Pk Hotel, Belfast, United Kingdom
E-mail: michael.grantham@concrete-solutions.info
Phone: 44-0-1843-606084
www.concrete-solutions.info

INTERNATIONAL COLLOQUIUM ON ARCHITECTURE STRUCTURE INTERACTION FOR SUSTAINABLE BUILT ENVIRONMENT

Date: November 18, 19 & 20, 2013
Venue: India Habitat Centre, Lodhi Road, New Delhi, India

Organised By
Structural Engineers World Congress (India)

Supported by
Ministry of Urban Development Government of India

In Association with
Indian Association of Structural Engineers (IAStructE)
Consulting Engineers Association of India (CEAI)

Media Partner
THE Masterbuilder
Nobody Covers Civil Engineering Better
MB Publishers Pvt. Ltd.

About the Colloquium

The Structural Engineers World Congress is dedicated to the Art, Science and Practice of Structural Engineering. The Colloquium focuses on the today's issues of global concern and aims to initiate a dialogue on the idea of creating a sustainable built environment. A galaxy of international stalwarts in Architecture and Structural Engineering are being brought together.

This Colloquium presents a unique and excellent opportunity for every professional involved in Architecture and Structural Engineering to interact with pioneers in their fields. It also provides a great forum to interact with fellow professionals, learn more about current practices and trends for the future.

About SEWC

SEWC aims to cover major aspects pertaining to technical and professional practice issues. The congress focuses on the needs and the con-temporary issues of the structural engineering profession worldwide and highlights the profession's interface with the society.

It also re-iterates the impact of the structural engineering profession on the society reflected by excellent public image, standing and credi-bility of structural engineers. SEWC presents excellent opportunities for structural engineering professionals to interact with each other and to learn more about what is happening in the World of Structural Engineering now and about the trends for the future.

Delegate Fee

Fee Categories	Early Fee before 15th October, 2013 (₹)	Standard Fee after 15th October, 2013 (₹)
Members of Supporting Organizations	8,000	10,000
Non Members	10,000	12,000
Spouse / Accompanying Person	4,000	5,000
Foreign Delegates	$ 400	$ 400
Bulk Reg. Discount for Orgs. Deputing#		
5-9 delegates#	Less 10%	Less 10%
10 & Above#	Less 20%	Less 20%
Students	1,500	2,000

Applicable upto November 5, 2013 only. Not valid for spot regs. *Student ID Card and Letter from their Educational Institution required. Some of the privileges mentioned above for delegates will not be available for students and accompanying persons

Stall Reservation Fee

Category A : **For Sponsors only**
Category B : Single Stalls : ₹ 25,000
Double Stall : ₹ 45,000
Category C : For Supporting Orgs. Only

Souvenir Advertisement Tariff

Gate Fold	₹ 1,00,000	Back Inside	₹ 40,000
Back Page	₹ 75,000	Full Page	₹ 25,000
Front Inside	₹ 50,000	Half Page	₹ 15,000

All Advertisements are in Colour

Sponsorship Opportunities

Principal Patron ₹ 10,00,000
Patron ₹ 7,50,000
Co-Patron ₹ 5,00,000
Sponsor ₹ 3,00,000
Co-Sponsor ₹ 2,00,000
Associate Sponsor ₹ 1,00,000
Supporting Organisation ₹ 50,000

SEWC Founding Organizations

Structural Engineering Institute of ASCE (SEI-ASCE)
Japan Structural Consultants Association (JSCA)
Institute of Structural Engineers [IstructE]
American Concrete Institute (ACI)
International Association of Shells and Spartial Structures (IASS)
Structural Engineers Association of California (SEAOC)

Address for Correspondence:

Mr. Shyam Najmi, Director, SEWC (I) Conference Secretariat,
CEAI Head Quarter, OCF Plot No. 2, Pkt 9, Sec B, Vasant Kunj, New Delhi-110070.
Mob: 91-98-1140 1507 | Ph: 91-11-26134644 | Fax: 91-11-26139658
Email: sewcindia2013@gmail.com; sewci2013@gmail.com; sewc2013@gmail.com
Web: www.sewc-worldwide.org


SELECTED
Superbrand
INDIA 2011/12
Consumer Validated
Strong enough to uphold
an Engineer's promise.
UltraTech
CEMENT
The Engineer's Choice
ADITYA BIRLA GROUP

STRUCTURAL ENGINEERING SEWC WORLDWIDE

International
JOURNAL of
SEWC
Structural Engineers World Congress